Article

An agonist radioligand for the proinflammatory lipid-activated G protein-coupled receptor GPR84 providing structural insights

Meryem Köse, Thanigaimalai Pillaiyar, Vigneshwaran Namasivayam, Elisabetta De Filippo, Katharina Sylvester, Trond Ulven, Ivar von Kügelgen, and Christa E Müller

J. Med. Chem., **Just Accepted Manuscript** • DOI: 10.1021/acs.jmedchem.9b01339 • Publication Date (Web): 13 Nov 2019

An agonist radioligand for the proinflammatory lipid-activated G protein-coupled receptor GPR84 providing structural insights

*Meryem Köse,[†,&] Thanigaimalai Pillaiyar,[†,&] Vigneshwaran Namasivayam,[†,&] Elisabetta De Filippo,[†] Katharina Sylvester,[†] Trond Ulven,[¥] Ivar von Kügelgen,[%] and Christa E. Müller[†,]**

[†]PharmaCenter Bonn, Pharmaceutical Institute, Department of Pharmaceutical and Medicinal Chemistry, University of Bonn, An der Immenburg 4, D-53121 Bonn, Germany.

[¥]Department of Drug Design and Pharmacology, University of Copenhagen, Universitetsparken 2, DK-2100 Copenhagen, Denmark.

[%]Pharma Center Bonn, Department of Pharmacology and Toxicology, Sigmund-Freud-Str. 25, D-53127 Bonn, Germany.

[&]Authors contributed equally

KEYWORDS: agonist, diindolylmethane, docking studies, G protein-coupled receptors, GPR84, homology modeling, medium-chain fatty acid, orphan GPCR, radioligand, structure-activity relationships, synthesis, uracil.

Abstract

The orphan G protein-coupled receptor (GPCR) GPR84 is expressed on immune cells mediating proinflammatory and immunostimulatory effects. In this study, we prepared the fully efficacious, non-biased GPR84 agonist 6-hexylamino-2,4(1*H*,3*H*)-pyrimidinedione (**6**) in tritium-labeled form ([^{3}H]PSB1584) by hydrogenation of a hexenyl-substituted precursor with tritium gas. The radioligand was characterized by kinetic, saturation, and competition assays using membranes of Chinese hamster ovary cells recombinantly expressing the human GPR84. [^{3}H]**6** reversibly labeled the receptor with high affinity (K_D 2.08 nM). Structurally diverse orthosteric and allosteric ligands, including newly designed and synthesized compounds, were studied in competition binding assays. A homology model of GPR84 was generated to perform docking studies rationalizing the experimental data. The radioligand was additionally used for labeling GPR84 in native cells and tissues. [^{3}H]**6** constitutes the first GPR84 agonist radioligand representing a powerful tool for this poorly investigated GPCR, which has potential as a future drug target.

Introduction

GPR84 is a proinflammatory G protein-coupled receptor (GPCR), which is highly expressed on cells of the immune system (*e.g.* neutrophils, macrophages) and is upregulated under inflammatory conditions.[1-7] GPR84 functions as an amplifier of inflammatory signaling by enhancing the release of proinflammatory mediators, such as TNFα and various interleukins.[7] Its activation results in G_i signaling leading to a reduction in cAMP production *via* inhibition of adenylate cyclase.[4] In addition, GPR84 has been described to signal through G_{12}/G_{13}, linking receptor function to Rho/Rac signaling and modulation of the cytoskeleton. In human macrophages, GPR84 activation was found to mediate G_i protein-dependent Erk1/2 and Akt phosphorylation as well as G_i-$\beta\gamma$-dependent PI_3 kinase activation and calcium mobilization.[6,8,9] So far, only limited data regarding its functional significance is available. However, recent studies confirm the involvement of GPR84 in metabolic regulation and inflammation and indicate its clinical relevance in various diseases. GPR84 was found to be involved in inflammatory processes relevant to gastroesophageal reflux disease,[10] inflammatory bowel disease,[11] multiple sclerosis,[5] neuropathic pain[12] and Alzheimer's disease.[13] Moreover, GPR84 has been linked to obesity and diabetes.[14-17] Preliminary evidence indicates that GPR84 might be associated with leukemogenesis,[18] osteoclastogenesis,[19] as well as organ fibrosis, a pathological outcome of many inflammatory and metabolic diseases.[20]

GPR84 was identified as a fatty-acid sensing receptor, being activated by micromolar concentrations of medium chain fatty acids (MCFAs) with chain lengths of C9-C14.[4] Decanoic acid (**1**) was described as the most potent MCFA with a moderate EC_{50} value of 4.5 μM. Several laboratories confirmed GPR84 activation by MCFAs and additionally by hydroxylated MCFAs.[7,21-25] Nevertheless, to date, it is still not fully accepted by the scientific community that the weakly potent MCFAs represent the endogenous agonists of GPR84. Due to the lack of potent ligands, comprehensive studies were hampered. Only recently, potent synthetic agonists have been

developed. The naturally occurring benzoquinone embelin (3-undecyl-2,5-dihydroxy-1,4-benzoquinone, **2**), a lipid-like molecule, also acts as a GPR84 agonist.[21,26,27] Subsequent structure-activity relationship study of **2** led to a new embelin analogue with 45-fold higher potency at human GPR84 than embelin itself.[8] The synthetic compound 6-octylaminouracil (**3**) was discovered as another surrogate GPR84 agonist by screening of a compound library.[7] High-throughput screening efforts by Zhang *et al*. resulted in the identification of 2-(hexylthio)-6-hydroxypyrimidin-4(3*H*)-one (**4**).[28] Further optimization of lead structure **4** resulted in the development of 6-nonylpyridine derivative **5**.[29] Lead compound **3** was optimized leading to the development of potent GPR84 agonists (e.g. compound **6** (6-hexylamino-2,4(1*H*,3*H*)-pyrimidinedione) and **7** (6-((*p*-bromo-phenylethyl)amino)-2,4(1*H*,3*H*)-pyrimidinedione).[24] A structurally very different GPR84 agonist is the natural product-derived 3,3'-diindolylmethane (DIM, **8**),[30] which had previously been described to activate the estrogen receptor[31] and the arylhydrocarbon receptor (AhR)[32] at micromolar concentrations (>5 μM). Subsequent studies confirmed the ability of **8** to activate human GPR84 with EC_{50} values between 0.5 to 5.9 μM.[4,22,24,25,28] DIM was proposed to bind to an allosteric site distinct from the decanoic acid binding site and to act as an ago-allosteric modulator activating the receptor by itself and also increasing the effects of lipidic and lipid-like agonists such as decanoic acid.[22,25,26] Starting from DIM as a lead structure, potent GPR84 agonists were developed, such as the agonist 3,3'-di-(5,7-difluoro-1*H*-indole-3-yl)methane (**9**, PSB-16671).[26] However, **9** appears to additionally interact with (an)other target(s).[33]

In contrast to agonists, the development of GPR84 antagonists has so far only been described in the patent literature.[34] In a recent study, antagonists from a patented series were reported as non-competitive antagonists, binding to a different binding site than the fatty acids and also different from that of 3,3'-diindolylmethane.[25] Structures and EC_{50} values of selected standard GPR84

agonists together with their potencies determined in different functional assay systems are summarized in Table 1.

Table 1. Potencies of selected standard GPR84 agonists determined in different assay systems

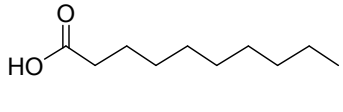

1 Decanoic acid

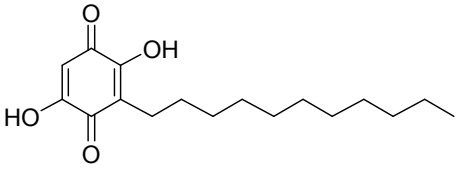

2 Embelin

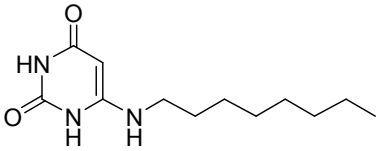

3 6-Octylaminouracil

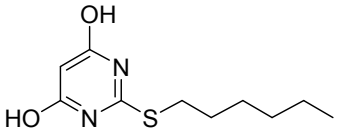

4 2-Hexylthiopyrimidine-4,6-diol

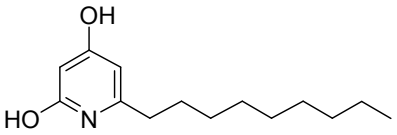

5 6-Nonylpyridine-2,4-diol

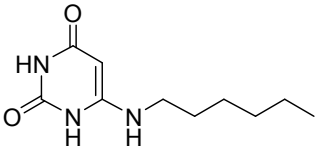

6 6-Hexylamino-2,4(1*H*,3*H*)-pyrimidinedione (**PSB-1584**)

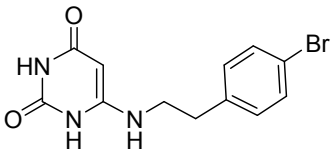

7 6-((*p*-Bromophenylethyl)amino)-2,4(1*H*,3*H*)-pyrimidinedione (**PSB-17365**)

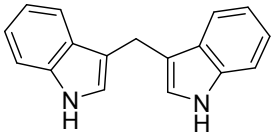

8 3,3'-Diindolylmethane (DIM)

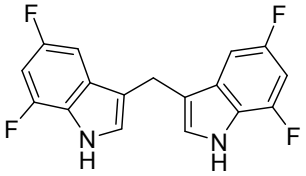

9 3,3'-Di-(5,7-difluoro-1*H*-indol-3-yl)methane (**PSB-16671**)

Standard GPR84 agonists	**Assay system**				
	cAMP assay EC_{50} (μM)	**[^{35}S]GTPγS assay** EC_{50} (μM)	**Calcium assay** EC_{50} (μM)	**IP assay**	**β-arrestin assay** EC_{50} (μM)
Decanoic acid (**1**)	**4.5**[a, 4] **7.42**[b,26] **20**[j,25] **48**[d,22]	**4.6**[a,4] **25**[j,25]	**48**[e,4] **30**[f,21]	n.d.	**6.08**[b,26] **10**[c,21]
Embelin (**2**)	**0.089**[c,8] **0.2**[j,25] **0.421**[a,21] **0.795**[b,26]	**0.63** [j,25]	**0.63**[h,21]	n.d.	**0.400**[b,26] **5.0**[b,21]
6-Octylaminouracil (**3**)	**0.0167**[b,24] **0.341**[c,28] **0.438**[c,29]	**0.512**[d,7]	**0.653**[g,29] **1.25**[g,28]	**0.105**[h, 7]	**0.114**[b,24] **1.75**[i,28]
2-Hexylthiopyrimidine derivative (**4**)	**0.001**[j,25] **0.134**[c,28] **0.144**[c,29]	**0.00079** [j,25]	**0.139**[g,29] **0.213**[g,28]	n.d.	**0.597**[i,28]

6-Nonylpyridine-2,4-diol (**5**)	**0.000352**[c,29]	n.d.	**0.000189**[g,29]	n.d.	n.d.
6-Hexylaminouracil (**6**)	**0.00493**[b,24]	n.d.	n.d.	n.d.	**0.00318**[b,24]
6-(*p*-Bromophenyl-ethylamino)uracil (**7**)	**0.00249**[b,24]	n.d.	n.d.	n.d.	**0.104**[b,24]
3,3'-Diindolylmethane (**8**)	**0.252**[b,26] **0.7**[a,4] **5.9**[d,22] **1.11**[c,28] **1.26**[j,25]	**0.5**[a,4] **1.0**[j,25] **11**[d,30]	n.d.	n.d.	**1.64**[b,26]
3,3'-Di-(5,7-difluoro-1*H*-indol-3-yl)methane (**9**)	**0.0413**[b,26]	n.d.	n.d.	n.d.	**5.47**[b,26]

[a]CHO/human GPR84 cells; [b]CHO/ß-arrestin2/human GPR84 cells. [c]HEK293/human GPR84 cells. [d]Sf9 insect/Gαi/human GPR84 cells. [e]CHO/aequorin reporter/$G_{\alpha16}$, G_{qs5}, G_{qo5}, and G_{qi9}/human GPR84 cells. [f]CHO/Gqi5/human GPR84 cells. [g]HEK293/Gα16/human GPR84 cells. [h]HEK/Gqi5/human GPR84 cells. [i]HEK293/β-arrestin2/human GPR84 cells. [j]Flp-In TREx 293-FLAG-human GPR84-eYFP cells. n.d., not determined.

As shown in Table 1, the determined agonist potencies in the different assay systems can vary considerably. For example, determined EC_{50} values for agonist **3** range between 0.0167 and and 0.438 μM (26-fold difference). It is well known that functional assays can be influenced by various factors. Receptor expression levels, ligand bias, activity of signaling cascades in specific cells, or nonspecific, receptor-independent effects can affect the measured EC_{50} values. Thus, values obtained in different functional test systems are not comparable.[35,36]

However, to date, only functional data are available, and so far, only two studies have been performed attempting to investigate the binding mode of agonists.[22,25] While Nicaido et al. created a homology model of GPR84 based on the active-state structure of the β_2-adrenoceptor,[22] Mahmud et al. generated a homology model using the transmembrane domain architecture of the orexin receptor type 1 (OX_1 receptor).[25] Moreover, mutagenesis studies were performed and the mutants were investigated in GTPγS assays investigating G protein activation.[22,25]

In addition to functional assays, radioligand binding studies would be an ideal basis for molecular modeling and docking studies. An antagonist GPR84 radioligand, [^{3}H]G9543, whose preparation was described in a patent,[34] and which had been utilized by Milligan et al., could neither be displaced by decanoic acid nor by DIM.[25] Consequently, [^{3}H]G9543 was supposed to bind to a third binding site distinct from the putative orthosteric binding site for fatty acids, and also different from the allosteric binding site for DIM. Thus, to date, it has not been possible to directly assess the binding affinities of standard GPR84 agonists. To address this issue, we prepared a high-affinity agonist GPR84 radioligand, which binds to the putative orthosteric, fatty acid binding site. In a previous study, we had shown that unlabeled **6** is a metabolically stable, highly potent and fully efficacious, non-biased agonist at human GPR84 as determined in cAMP (EC_{50} 4.93 nM) and β-arrestin (EC_{50} 3.18 nM) assays.[24] We selected this compound for tritium labeling to obtain the first agonist radioligand for GPR84. The radioligand was fully characterized and applied in competition binding assays. The determined binding data served as a basis for analyzing interactions of ligands with GPR84 studied by docking of compounds into a receptor homology model.

Results and discussion

Chemistry. The radioligand [^{3}H]**6** was prepared as depicted in Scheme 1. *N*-Hexenylphthalimide (**12**) was synthesized by Mitsunobu reaction from commercially available phthalimide (**10**) and (*E*)-hex-2-enol (**11**) in the presence of diethyl azodicarboxylate (DEAD) and triphenylphosphine.[37] Compound **12** was converted to the amine **13** using hydrazine hydrate under reflux conditions. Amine **13** was subsequently reacted with 6-chlorouracil (**14**) under reflux[38] to afford the desired radioligand precursor (*E*)-6-(hex-2-en-1-ylamino)pyrimidine-2,4(1*H*,3*H*)-dione (**15**). The catalytic hydrogenation procedure was initially investigated with non-radioactive hydrogen gas to prepare non-radioactive **6**, before radiolabeling was approached. In procedure A, the reaction was performed at 25 psi (1.7 bar) in methanol (MeOH) : tetrahydrofuran (THF) (1:1) in the presence of

10% palladium on activated charcoal for 2 h at room temperature. In procedure B, the reaction was performed at 35 psi (2.4 bar) in *N*,*N'*-dimethylformamide (DMF) : THF (1:1) as a solvent instead. Under both conditions, **15** was completely hydrogenated to product **6**. The alkene **15** was subsequently custom-labeled *via* hydrogenation of the double bond with tritium gas to obtain the desired radioligand [^{3}H]**6**, whose identity was confirmed by mass spectrometry. [^{3}H]**6** displayed a specific activity of 60 Ci/mmol (2.22 TBq/mmol) and a radiochemical purity of 99.8% as determined by HPLC−UV (254 nm). (see Figures S1-S3).

Scheme 1. Preparation of the GPR84 agonist radioligand [^{3}H]**6**[a]

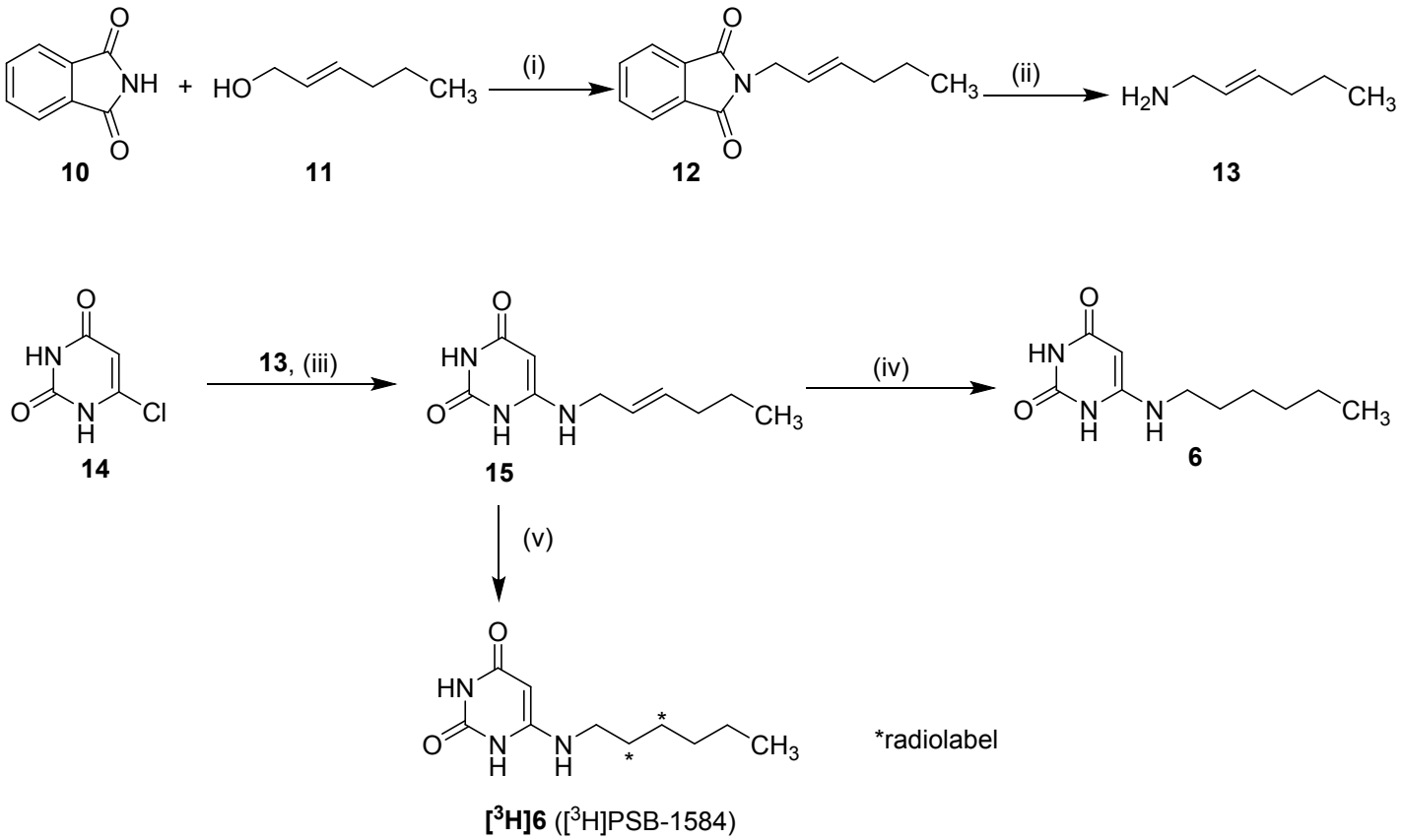

[a]**Reagents and conditions**: (i) PPh_3, $EtO_2CN{=}NCO_2Et$, THF, 0 °C to rt, 12 h, 95%; (ii) hydrazine hydrate solution (~80% in H_2O), 100 °C, 3 h, 75.6%; (iii) 1-butanol, 125 °C, 12 h, 91%; (iv) procedure A: MeOH:THF (1:1), Pd/C (10%), H_2, 1.7 bar, 2 h, 98%; procedure B: *N*,*N'*-

dimethylformamide (DMF):THF (1:1), Pd/C (10%), H_2, 2.4 bar, 2 h, 97.5%; (v) custom labeling in THF as a solvent (for details see SI).

A large number of previously described GPR84 ligands[4,8,24,25,26,27] were subsequently studied in binding assays using the new radioligand. In addition, we synthesized three series of new lipid-like compounds (Scheme 2). Pyrimidine derivatives **4**, **62**-**68**, **73**-**77** and **79**-**85** were prepared from 6-hydroxy-2-thioxo-2,3-dihydropyrimidin-4(1*H*)-one (**61**), 4-hydroxy-pyrimidine-2(1*H*)-thione derivatives (**69**-**71**), or 2-thiopyrimidine-4-carboxylic acid (**72**), respectively, by alkylation with (aryl)alkyl bromides in the presence of potassium carbonate in methanol under reflux conditions. Carboxylic acid ester **76** was hydrolyzed in the presence of 2-N sodium hydroxide to produce the corresponding carboxylic acid **77**. Orotic acid ester and amide derivatives were synthesized from orotic acid (**78**) as depicted in Scheme 2. For preparing the orotic acid esters **79** and **80**, compound **78** was dissolved in butanol or hexanol and refluxed for 12 h in the presence of catalytic amounts of concentrated sulfuric acid. Orotic acid amides were obtained by condensation of **78** with various amines in the presence of *O*-(7-azabenzotriazol-1-yl)-*N*,*N*,*N*′,*N*′-tetramethyluronium-hexafluorophosphate (HATU) and triethylamine (TEA) in DMF.

Scheme 2. Synthesis of **4**, **62**-**68**, **73**-**77** and **79**-**85**[a]

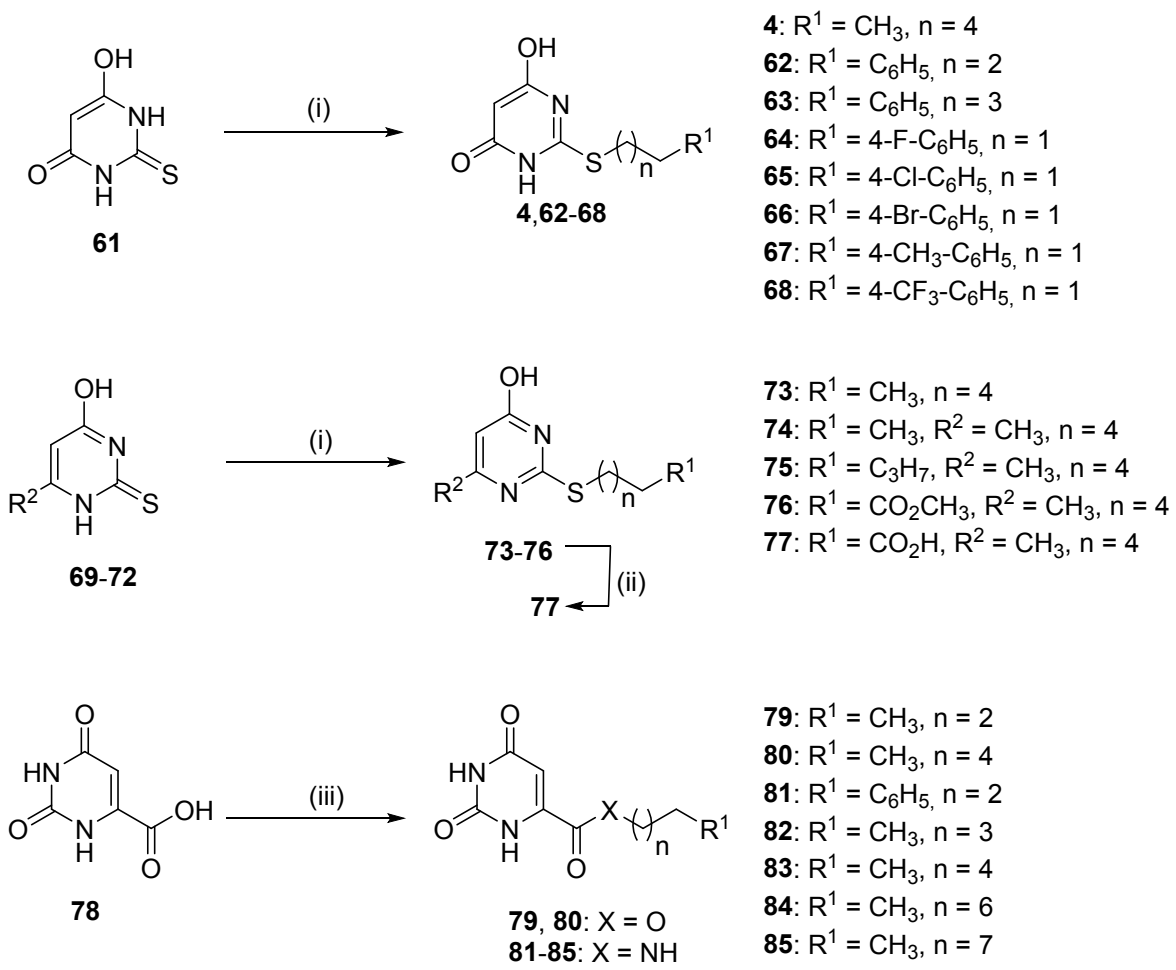

[a]**Reagents and conditions:** (i) K_2CO_3, methanol, reflux, 12 h; (ii) from **76**, 2 N NaOH, methanol, 80 °C, 1 h; (iii) for esters (X = O): alcohols, H_2SO_4, reflux, 12 h; for amides (X = NH): amines, HATU, TEA, DMF, 12 h, rt.

Biological experiments

Pharmacological characterization of the new radioligand. Membrane preparations of a CHO cell line stably transfected with the human GPR84 (CHO-hGPR84) were used to establish a radioligand binding assay. In preliminary experiments, specific binding of 3-10 nM of [^{3}H]**6** to GPR84-expressing cells was detected, while only negligible binding to non-transfected CHO cells

was observed under the same conditions (see Figure S4). Subsequently, we investigated the effects of the buffer composition on [^{3}H]**6** binding (1 nM). The addition of 0.05 % of fatty acid-free bovine serum albumin (BSA) to tris(hydroxylmethyl)aminomethane (TRIS) as an incubation buffer significantly increased specific binding (8-fold, 0.0024, **). The addition of $MgCl_2$ (10 mM) also increased specific binding by 3-fold. Therefore, we combined both, $MgCl_2$ and BSA, which led to a further significant increase in specific binding (Figure 1). In contrast, the addition of NaCl led to a significant decrease in specific binding while the IC_{50} value of agonist **6** was not affected (Figure 1 and Figure S5). Sodium ions are known to act as negative allosteric modulators of many GPCRs.[38] In contrast, Mg^{2+} ions may promote the formation of a high-affinity agonist-receptor-G protein complex acting as a positive allosteric modulator. The same effect had been observed in previous studies with agonist radioligands, *e.g.* for GPR35 and GPR17.[39-42]

Thus, 50 mM TRIS buffer, pH 7.4 containing 10 mM $MgCl_2$ and 0.05 % fatty acid-free BSA was found to be the optimal assay buffer resulting in low non-specific binding of only 15%, and these conditions were therefore used in all subsequent binding assays.

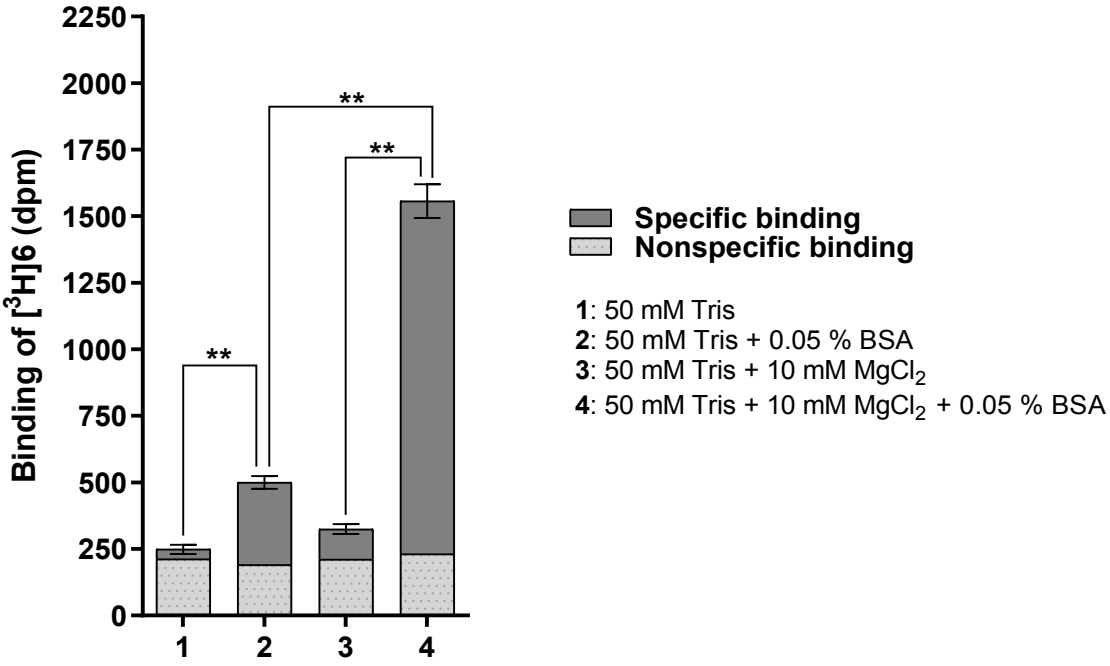

Figure 1. Effects of BSA and cations on [^{3}H]**6** binding. The experiments were performed at 25 °C (150 min) using 1 nM [^{3}H]**6** and 10 µg of a membrane preparation of CHO cells expressing the human GPR84 (CHO-hGPR84 cells). Data represent means of two independent experiments performed in duplicate; dpm, decays per minute. The unpaired t-test was used for statistical comparisons (**, $p<0.01$).

As a next step, kinetic studies with CHO-hGPR84 cell membranes (10 µg of protein) were performed using 1 nM [^{3}H]**6** in 50 mM TRIS buffer, pH 7.4, supplemented with 10 mM $MgCl_2$ and 0.05 % BSA. Both association and dissociation appeared monophasic (Figure 2A/B). In the association experiments ($t_{1/2}$ = 21 min) an equilibrium was reached within less than 120 min which remained stable for at least 6 h indicating that an incubation time of 150 min is sufficient to ensure equilibrium binding of [^{3}H]**6**. The binding was reversible after the addition of a high concentration (100 µM) of the potent GPR84 agonist **7**[24] with a dissociation half-life of 32 min (Figure 2B). A

kinetic K_D value of 2.04 nM was calculated. In saturation experiments using 12 different radioligand concentrations ranging from 0.04 to 10 nM, a K_D value of 2.08 nM and an apparent B_{max} value of 1.87 pmol/mg protein were determined (Figure 2C). We subsequently transferred the assay to a 96-well plate format, which allows a higher throughput than the originally used single vials. A radioligand concentration of 2 nM [^{3}H]**6** was found to be suitable for performing competition binding assays in a 96-well plate format. The nonspecific binding at that concentration amounted less than 7 % of total binding. Homologous competition experiments with the unlabeled ligand **6** were performed using a high concentration of GPR84 ligand **7** (10 μM) to determine non-specific binding. Homologous competition assays for agonist **6** revealed a K_i value of 2.98 nM (Figure 2D). Thus, all three determined affinity values, K_i for the unlabeled agonist **6**, the kinetic K_D value, as well as the K_D value of [^{3}H]**6** obtained in saturation assays, were virtually identical.

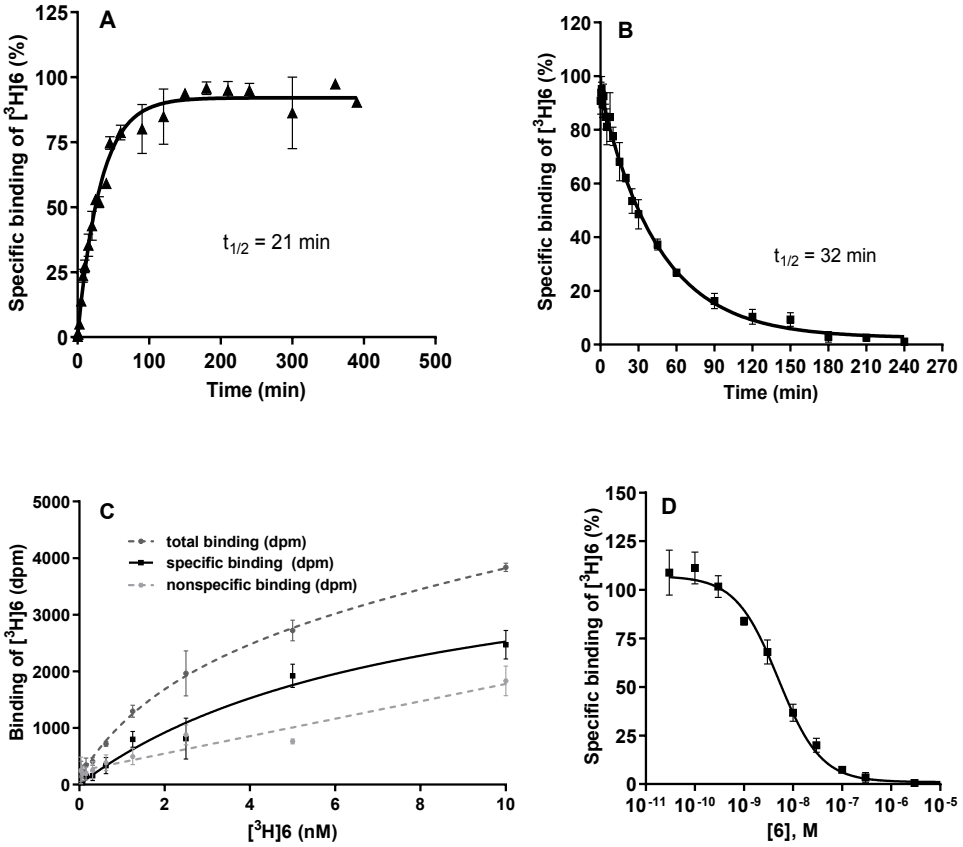

Figure 2. (A) Association and (B) dissociation curve of [^{3}H]**6** binding (1 nM) at 25 °C to membrane preparations of CHO-human GPR84 cells (10 µg protein/vial). Dissociation was achieved by addition of the GPR84 agonist **7** (100 µM) after 150 min of pre-incubation. A kinetic K_D value of 2.04 nM was determined. (C) Saturation curve of binding of increasing concentrations of [^{3}H]**6**; experiments were performed at 25 °C with 10 µg of protein per vial. For the determination of nonspecific binding, 10 µM of **7** was used. The following binding parameters were calculated: $K_D = 2.08 \pm 0.68$ nM, $B_{max} = 1.87 \pm 0.19$ pmol/mg protein. (D) Homologous competition experiments. A K_i value of 2.98 ± 0.38 nM was determined for **6** (see Table 2). Mean values ± SEM from 3-6 independent experiments performed in duplicates are shown.

Binding affinity of standard GPR84 ligands. With the optimized radioligand-binding assay, we initially investigated the standard GPR84 agonists **1**-**4** and **6**-**9** in competition experiments (for K_i values see Table 2-5). As expected, compounds **1**-**4**, **6** and **7** with a lipid-mimetic structure were able to completely displace the radioligand (Figure 3). The determined K_i values were lower than the EC_{50} values previously determined in functional assays (for previously determined EC_{50} values see Table 1). Decanoic acid (**1**) and embelin (**2**) both showed a higher affinity (K_i 1780 nM and 23.6 nM, respectively) in binding assays compared to the previously determined potencies in functional assays (3- to 14-fold for **1** and 8- to 212-fold for **2**). Agonist **3** displayed a K_i value of 0.626 nM in the binding studies, which is 27- to 2800-fold lower than the respective EC_{50} values determined in functional assays (see Table 1). Similarly, **4** (K_i 0.219 nM) displayed a 5- to 2730-fold higher affinity in binding studies compared to the potency measured in functional studies. Interestingly, the K_i value for **6** (2.98 nM) corresponded very well with the EC_{50} values previously determined in cAMP and β-arrestin assays (4.93 nM and 3.18 nM, respectively). In contrast, the K_i value of **7** (0.317 nM) was 8- to 330-fold lower than the published EC_{50} values for **7**.

DIM (**8**) did not lead to an inhibition but to a concentration-dependent increase in the specific binding of [^{3}H]**6** by up to 100 % compared to the control in the absence of DIM (Figure 3). Although previous studies had suggested that **8** may be an ago-allosteric modulator,[22,25,26] it has not been possible so far to study direct receptor-ligand interaction for DIM. Here we directly show for the first time that **8** indeed binds to a different site than the lipid mimetic [^{3}H]**6**. The observed increase in specific binding of [^{3}H]**6** further suggests that **8** not only activates the receptor, but at the same time, it positively modulates the binding of the lipid mimetic **6**, which is presumed to act as an orthosteric GPR84 agonist. This observation is in agreement with previously reported cAMP data showing an increase in efficacy and potency for decanoic acid with increasing concentrations of **8**.[26]

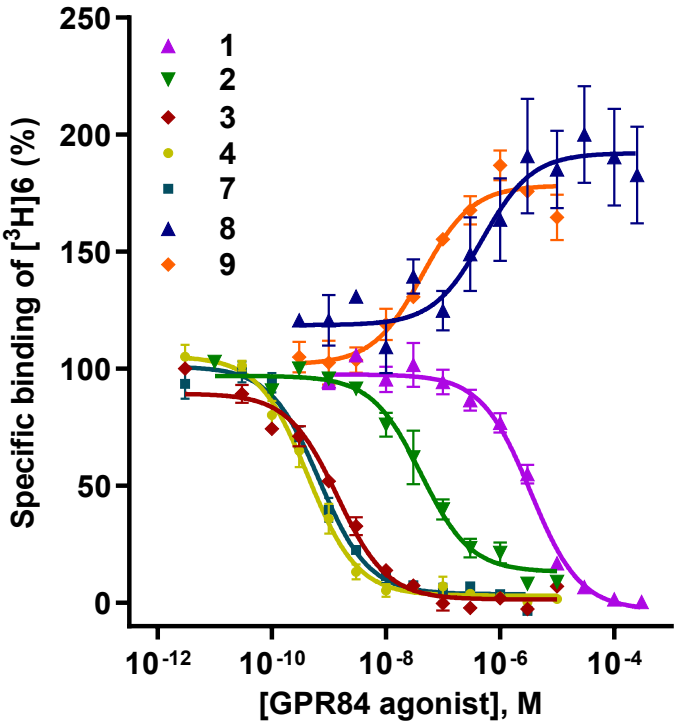

Figure 3. Competition binding experiments for standard agonists versus the agonist radioligand [^{3}H]**6**. The experiments were performed as described in the Experimental section. K_i values for lipid-like agonists were as follows: 1780 ± 285 nM for **1** (decanoic acid), 23.6 ± 6.8 nM for **2**

(embelin), 0.626 ± 0.205 nM for **3** (6-octylaminouracil), 0.219 ± 0.054 nM for **4** (2-hexylthiopyrimidine derivative), and 0.317 ± 0.033 nM for **7** (6-(*p*-bromophenylethylamino)uracil). For positive allosteric modulators, EC_{50} values were as follows: 368 ± 42 nM for **8** (diindolylmethane) and 41.5 ± 7.0 nM for **9** (5,5',7,7'-tetrafluoro-DIM). Data points represent means ± SEM from 3-6 independent experiments, each performed in duplicates.

Binding affinities of medium-chain (hydroxy)fatty acids. Next, we investigated several medium-chain (hydroxy)fatty acids (C8-C14, (hydroxy)MCFAs) in binding assays at GPR84 (Table 2). In parallel, we also evaluated these MCFAs in functional assays (cAMP and β-arrestin assays).

Table 2. Binding affinities and functional potencies and efficacies of (hydroxy)fatty acids at the human GPR84

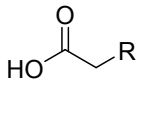

Structure A (**1**, **16-20**)

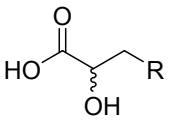

Structure B (**21**, **22**)

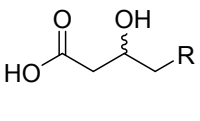

Structure C (**23-26**)

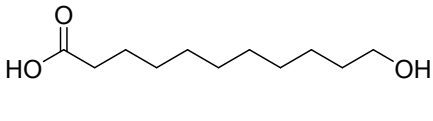

Structure D (**27**)

Compound	**R**	**Human GPR84**		
		Radioligand binding assay **K_i ± SEM** (μM) vs. [^{3}H]**6** (or percent inhibition ± SEM at 100 μM) (n=3)[a]	**cAMP assay** **EC_{50} ± SEM** (μM) (or percent receptor activation at 100 μM) [*efficacy*][b] (n=3)[a]	**β-Arrestin assay** **EC_{50} ± SEM** (μM) (or percent receptor activation at 100 μM) [*efficacy*][c] (n=3)[a]
Embelin (**2**) (for structure see **Table 1**)		**0.0236** ± 0.0068	**0.795** [*86* %][26]	**0.400** [*100* %][26]
Structure A: Fatty acids				

Octanoic acid (**16**)	C_6H_{13}	**19.6** ± 6.8	> **100** (36 %)	> **100** (2 %)[d]
Decanoic acid (**1**)	C_8H_{17}	**1.78** ± 0.29[f]	**7.42** [*100 %*][26]	**6.08** [*92%*][26]
Undecanoic acid (**17**)	C_9H_{19}	**0.108** ± 0.024	**1.60** ± 0.14 [*93 %*][e]	**4.36** ± 1.51 [*82 %*][e]
Dodecanoic acid (**18**)	$C_{10}H_{21}$	**2.17** ± 0.24	**8.87** ± 0.75 [*94 %*]	**3.49** ± 0.56 [*92 %*][e]
Tridecanoic acid (**19**)	$C_{11}H_{23}$	**1.93** ± 0.80	**9.61** ± 1.25 [*51 %*]	**1.70** ± 0.64 [*77 %*][d]
Tetradecanoic acid (**20**)	$C_{12}H_{25}$	**2.64** ± 0.63	**11.4** ± 1.6 [*63 %*]	**7.01** ± 3.20 [*61 %*][e]
Structure B: 2-Hydroxy-fatty acids				
(*R,S*)-2-Hydroxy-octanoic acid (**21**)	C_5H_{11}	≈ **100** (50 %)	**> 100** (17 %)	**> 100** (5%)
(*R,S*)-2-Hydroxy-tetra-decanoic acid (**22**)	$C_{11}H_{23}$	**0.318** ± 0.070	**3.86** ± 1.00 [*102 %*]	**4.36** ± 1.42 [*101 %*]
Structure C: 3-Hydroxy-fatty acids				
(*R,S*)-3-Hydroxy-decanoic acid (**23**)	C_6H_{13}	**3.31** ± 0.81	**31.8** ± 4.67 [*97 %*]	**4.05** ± 1.35 [*54 %*]
(*R,S*)-3-Hydroxy-do-decanoic acid (**24**)	C_8H_{17}	**0.110** ± 0.021	**1.31** ± 0.15 [*112 %*]	**3.25 ±** 1.34 [*125 %*]
(*R,S*)-3-Hydroxy-tetra-decanoic acid (**25**)	$C_{10}H_{21}$	**0.511** ± 0.107[e]	**1.57** ± 0.47 [*88 %*]	**0.432** ± 192 [78 %][d]
(*R*)-3-Hydroxy-tetra-decanoic acid (**26**)	$C_{10}H_{21}$	**0.472** ± 0.120	**1.75** ± 0.62 [*91 %*][e]	**0.452** ± 0.158 [*77 %*]
Structure D: 12-Hydroxydodecanoic acid				
(*R,S*)-12-Hydroxy-do-decanoic acid (**27**)	See struct. D	**> 10** (5 %)	> **100** (27 %)	**> 100** (-17 %)[d]

[a]Unless otherwise noted
[b]Efficacy [E_{max}] relative to the max. effect of decanoic acid (100 µM) (= 100%).
[c]Efficacy [E_{max}] relative to the max. effect of embelin (10 µM) (= 100%).
[d]n=2; [e]n=4; [f]n=7.

Undecanoic acid showed the highest binding affinity among the tested MCFAs with a K_i value of 108 nM (see Table 2 and Figure S6). It was also the most potent fatty acid in cAMP assays (EC_{50} 1.60 µM). Fatty acids with a shorter or a longer chain length displayed lower binding affinities ranging between 2-20 µM. We detected a K_i value of 19.6 µM for octanoic acid although no activity in cAMP and β-arrestin assays at concentrations up to 100 µM could be observed for this fatty acid. In previous studies, octanoic acid had also been shown to be inactive in functional assays.[4,7] In

general, we observed a high correlation between K_i values determined in binding studies and the EC_{50} values determined in cAMP accumulation studies using the same cell line (see Table 2 and Figure 4, $R^2 = 0.906$), while correlation with EC_{50} values obtained from β-arrestin assays appeared to be much lower ($R^2 = 0.621$). Previously, it had been difficult to predict the true binding affinities of GPR84 agonists. The herein determined binding affinity for decanoic acid (1.78 μM), for example, is 100-300 higher than the predicted affinity (K_A 170-530 μM) based on functional data.[25] For tetradecanoic acid, a very high EC_{50} value of 93.2 μM[4] or even no activity[7] had been reported in previous studies. In contrast, we determined a K_i value of 2.64 μM in binding assays. Using the same CHO cell line that overexpresses the human GPR84, the EC_{50} values were 11.4 μM (cAMP assay) and 7.01 μM (β-arrestin assay), respectively. These data illustrate, that functional data for agonists are highly dependent on the test system, e.g. on receptor expression levels, whereas binding data are largely independent and provide "true" affinities.

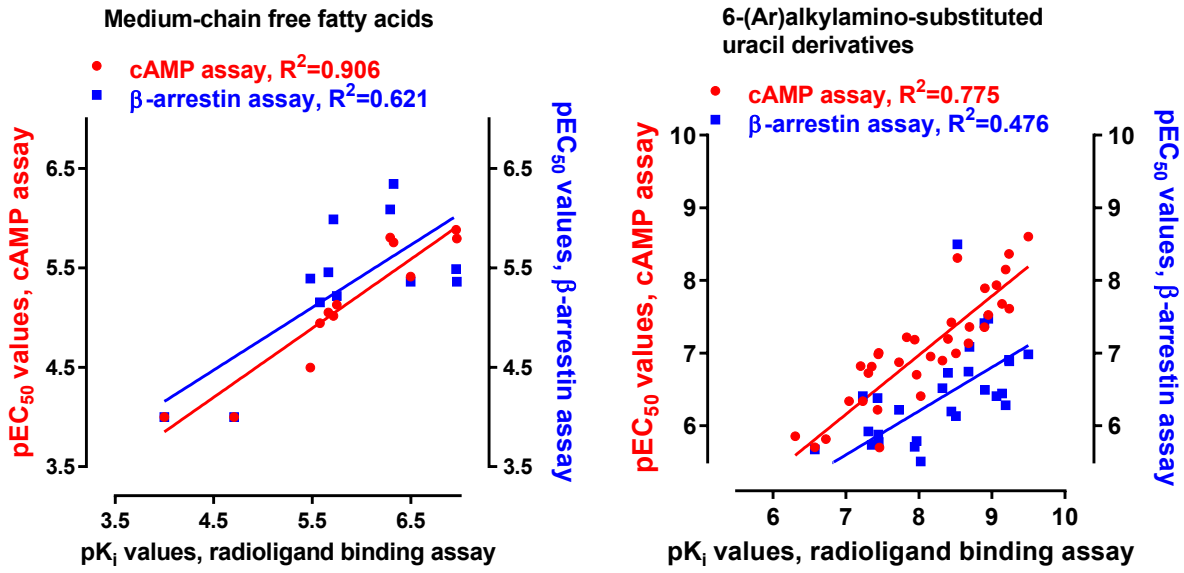

Figure 4. Correlation of pEC_{50} values of test compounds determined in cAMP assays (●) or β-arrestin assays (■) versus their respective pK_i values determined in radioligand binding assays. The same cell line (CHO-β-arrestin-human GPR84 cells) was used for all assays. R^2 was determined in a two-tailed Pearson test. **A**. fatty acid derivatives; **B**. 6-(ar)alkylamino-substituted uracil derivatives.

All hydroxyfatty acids, except for (*R*,*S*)-3-hydroxy-decanoic acid (**23**), showed higher binding affinities than the respective non-hydroxylated fatty acids confirming previous results from functional assays reported by Suzuki *et al*.[7] The position of the hydroxyl group, at C2 or C3, did not significantly affect the binding affinity (compare **22** and **25**).

Binding affinities of 6-(ar)alkylamino-substituted uracil derivatives. Next, a series of 6-(ar)alkylamino-substituted uracil derivatives (**28-60**) previously synthesized in our group[24] were tested for their binding affinity to the human GPR84 (for selected curves see Figure 5A, for K_i values see Table 3). As depicted in Figure 4B, the binding affinities correlated with the agonist potencies previously determined in cAMP assays (r^2=0.775), but much less with pEC_{50} values determined in β-arrestin assays (r^2=0.476) (for the previously obtained functional data see Table S2). As seen for the standard agonists **1-4**, **6** and **7**, binding affinities were up to 57-fold (cAMP assay, on average 17-fold) or up to 803-fold (β-arrestin assay, on average 161-fold) higher compared to their respective potencies in functional assays.

Table 3. Affinities of agonists at the human GPR84 determined in radioligand binding assays.

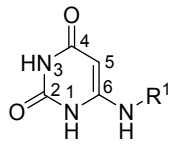 Structure A (**6**,**28**-**49**)	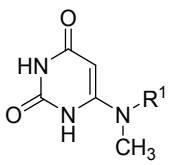 Structure B (**50**,**51**)	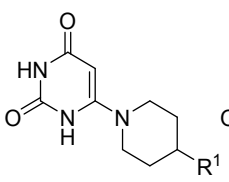 Structure C (**52**)	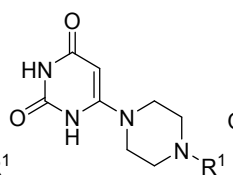 Structure D (**53**-**55**)	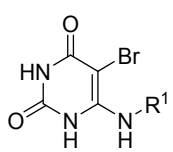 Structure E (**56**,**57**)	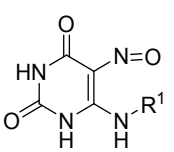 Structure F (**58**-**60**)

Compd.	**R^1**	**Human GPR84 Radioligand binding assays**[a] **K_i** ± SEM (μM) vs. [^{3}H]**6** (n=3)[b]
Structure A: 6-(Aryl)alkylaminouracils		
28	-$CH_2(CH_2)_3$-CH_3	**0.0910** ± 0.0080
6 (PSB-1584)	-$CH_2(CH_2)_4$-CH_3	**0.00298** ± 0.00038[c]
29	-$CH_2(CH_2)_5$-CH_3	**0.000866** ± 0.000204
3 (6-octylaminouracil)	-$CH_2(CH_2)_6$-CH_3	**0.000626** ± 0.000205
30	-$CH_2(CH_2)_7$-CH_3	**0.00112** ± 0.00007
31	-$CH_2(CH_2)_8$-CH_3	**0.000726** ± 0.000076
32	-$CH_2(CH_2)_6$-OH	**0.267** ± 0.016
33	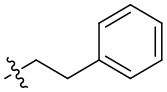	**0.0108** ± 0.0022
34	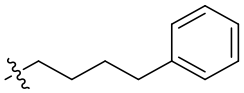	**0.000580** ± 0.000176
35	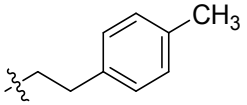	**0.00125** ± 0.00021
36	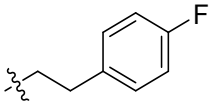	**0.0114** ± 0.0008
37	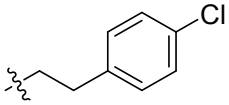	**0.000650** ± 0.000038
7 (PSB-17365)	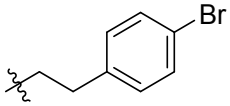	**0.000317** ± 0.000033

38	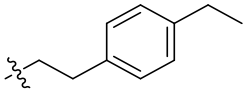	**0.000582** ± 0.000063
39	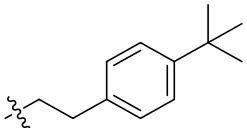	**0.00127** ± 0.00043
40	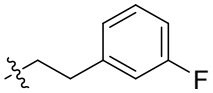	**0.00948** ± 0.00201
41	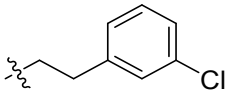	**0.00475** ± 0.00079
42	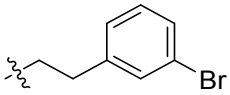	**0.00399** ± 0.00061
43	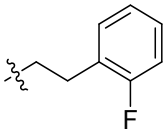	**0.0356** ± 0.0090
44	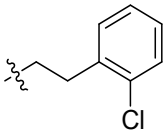	**0.0360** ± 0.0032
45	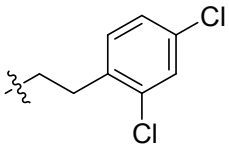	**0.00203** ± 0.00018
46	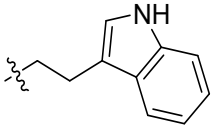	**0.497** ± 0.032
47	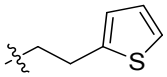	**0.0494** ± 0.0072
48	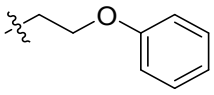	**0.00312** ± 0.00071
49	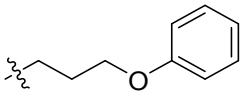	**0.00210** ± 0.00018
Structure B: **N^6-Methyl-substituted uracil derivatives**		
50	-$CH_2(CH_2)_4$-CH_3	**0.00694** ± 0.00031

51 Y-364	-$CH_2(CH_2)_6$-CH_3	**0.00360** ± 0.00047
Structure C		
52 Y-573	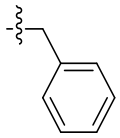	**0.0187** ± 0.0021
Structure D		
53	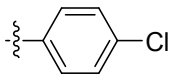	**0.0444** ± 0.0049
54 Y-617	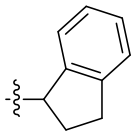	**0.0147** ± 0.0028
55	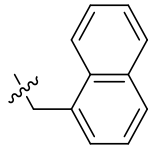	**0.0627** ± 0.0019
Structure E		
56	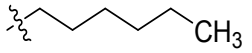	**0.225** ± 0.011
57 Y-373	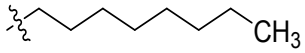	**0.0347** ± 0.0100[d]
Structure F		
58	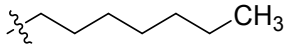	**0.0586** ± 0.0140
59 Y349	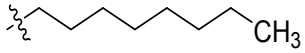	**0.0370** ± 0.0129
60	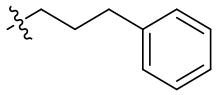	**0.189** ± 0.052

[a]Affinities were determined in competition binding experiments using 2 nM [^{3}H]**6** and membrane preparations of CHO cells recombinantly expressing hGPR84. [b]Unless otherwise noted. [c]n=6; [d]n=4.

Interestingly, for compound **6**, previously determined as the most potent unbiased GPR84 agonist of the series,[24] no significant difference between the K_i value and the EC_{50} values in both functional assays was observed (K_i 2.98 nM and EC_{50} 4.93 nM, respectively). In contrast, **37**, previously

determined as the most potent G_i-biased GPR84 agonist of the series, showed the highest difference (803-fold) between its K_i value from radioligand binding (0.650 nM) and its EC_{50} value determined in β-arrestin assays (EC_{50} 522 nM).

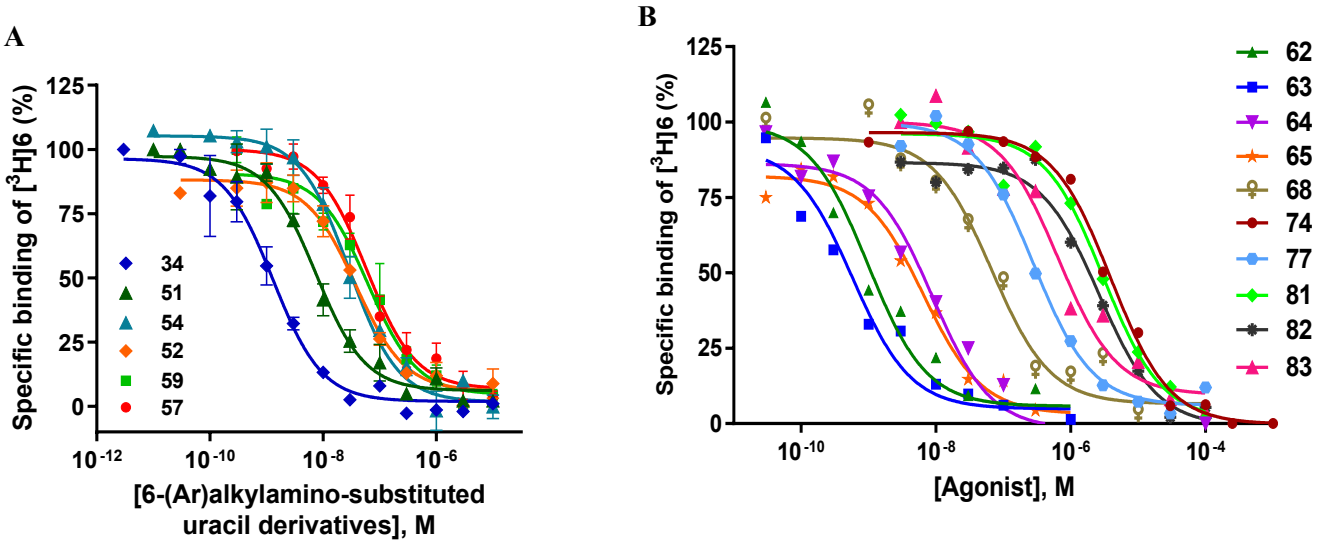

Figure 5. Competition binding experiments at membrane preparations of recombinant CHO cells expressing human GPR84. **A**. Competition binding curves for selected 6-(ar)alkylamino-substituted uracil derivatives. **B**. Competition binding curves for synthesized lipid-like compounds **62-65**, **68**, **74**, **77**, **81-83**. Data points represent means ± SEM from 3 independent experiments, each performed in duplicates. For K_i values see Table 4.

Binding affinities of thiopyrimidones and tetrahydropyrimidine carboxylic acid esters and amides. Taking the potent GPR84 agonist **4** (2-(hexylthio)-6-hydroxypyrimidin-4(3*H*)-one).[28] as a lead structure, we prepared a small series of derivatives and analogues and evaluated them in radioligand binding assays for their GPR84 affinity (for selected curves see Figure 5B, for K_i values see Table 4). Agonist **4** itself displayed a K_i value of 0.219 nM and was actually the compound with the highest affinity of all investigated GPR84 ligands. 6-Nonylpyridine-2,4-diol (**5**) previously

described to be even more potent than **4**,[28] was found to display 7-fold lower affinity as compared to **4** in binding studies (K_i 1.56 nM). 6-Octylaminouracil (**3**, 0.626 nM) and 6-*p*-bromophenethylaminouracil (**7**, 0.317 nM) belong to the compounds with the highest GPR84 affinity being similarly potent as **4**, while the affinity of 6-hexylaminouracil (**6**, 2.98 nM) is slightly lower. The rank order of potency of lipophilic agonists was generally somewhat different in radioligand binding assays as compared to functional assays. One reason could be due to difficulties in handling highly lipophilic, poorly water-soluble molecules. In binding assays employing cell membrane preparations, a higher percentage of DMSO can be used than in cellular systems, and predilutions can all be made in DMSO rather than aqueous buffer. Predilution in buffer could lead to a loss of compound resulting in reduced concentrations in the assay. Therefore, according to our experience, these data obtained in binding studies are most reliably representing true affinities.

Introducing aromatic residues into the alkyl chain of lead structure **4** was well tolerated leading to analogs with similarly potent affinity, e.g. 6-phenylethylthiopyrimidine-2,4-diol (**62**, K_i 0.700 nM), 6-phenylpropylthiopyrimidine-2,4-diol (**63**, 0.324 nM), and *p*-chlorobenzylthiopyrimidine-2,4-diol (**65**, 2.63 nM).

Deletion or replacement of the 4-hydroxy/oxo-function by hydrogen, alkyl or carboxylate in compounds **73**-**77** abolished or dramatically reduced GPR84 affinity. Replacement of the amino group in 6-(ar)alkylaminouracils by an ester or amide linker (compounds**79**-**85**) was also not well tolerated (Table 4).

Table 4. Affinities of agonists at the human GPR84 determined in radioligand binding assays

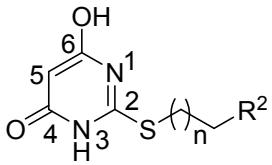

Structure A
4, 62-68

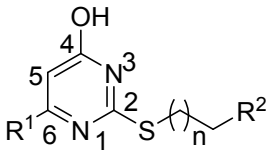

Structure B
73-77

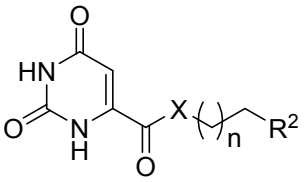

Structure C
79,**80**: X = O
81-85: X = NH

Compd.	n	R^1	R^2	Human GPR84 Radioligand binding assays[a] K_i ± SEM (μM) vs. [^{3}H]**6** (n=3)
Structure A				
1 (Decanoic acid, also see Table 1))				**1.78** ± 0.29
4[b] (2-(Hexylthio)-6-hydroxypyrimidin-4(3*H*)-one), also see Table 1)				**0.000219** ± 0.000054
5 (6-Nonylpyridine-2,4-diol, also see Table 1)				**0.00156** ± 0.00037
62	2	-	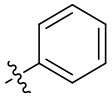	**0.000700** ± 0.000322
63[29]	3	-	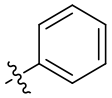	**0.000324** ± 0.000090
64	1	-	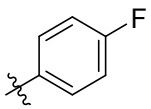	**0.00377** ± 0.00107
65	1	-	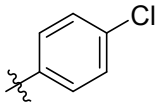	**0.00263** ± 0.00050
66	1	-	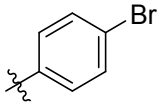	**0.00317** ± 0.00119
67	1	-	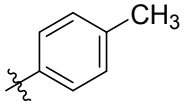	**0.00328** ± 0.00043
68	1	-	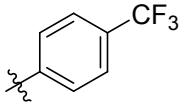	**0.0367** ± 0.0087
Structure B				

73	4	H	CH_3	**3.47** ± 0.65
74	4	CH_3	CH_3	**3.63** ± 1.56
75	4	C_3H_7	CH_3	**≥100** (51 %)
76	4	CO_2CH_3	CH_3	**>10** (9 %)
77	4	CO_2H	CH_3	**0.145** ± 0.052[c]
Structure C				
79	2	-	CH_3	**> 10** (-3 %)
80	4	-	CH_3	**1.21** ± 0.22
81	2	-	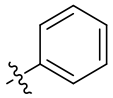	**1.59** ± 0.43[c]
82	3	-	CH_3	**1.56** ± 0.25[c]
83	4	-	CH_3	**0.469** ± 0.197[c]
84	6	-	CH_3	**>10** (12 %)
85	7	-	CH_3	**>10** (26 %)

[a]Affinities were determined in competition binding experiments using 2 nM [^{3}H]**6** and membrane preparations of CHO cells recombinantly expressing human GPR84. [b]Compound **4** was resynthesized and the synthetic procedure is described in the experimental section. [c]n=2.

Binding affinities of diindoylmethane derivatives. We further selected a series of diindolylmethane derivatives (compound **86-103**) that were previously shown to activate GPR84 in cAMP accumulation and/or β-arrestin recruitment assays.[26] Like DIM (**8**) itself (Figure 3), most of the substituted DIM derivatives and analogs also showed a concentration-dependent increase in specific binding of [^{3}H]**6** (for selected curves see Figure 6, for K_i values see Table 5).

Table 5. Affinity of 3,3'-diindolylmethane derivatives at the human GPR84

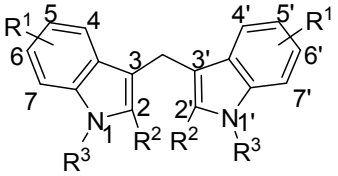

Structure A
(**8**,**9** **86**-**98**)

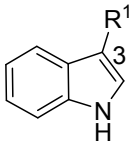

Structure B
(**99**-**101**)

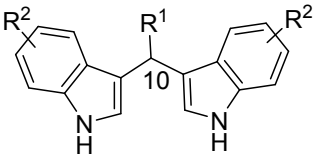

Structure C
(**102**,**103**)

Compd.	**R¹**	**R²**	**R³**	**Human GPR84 radioligand binding assays**[a] **EC_{50} (or IC_{50})**[b] ± SEM (μM) vs. [^{3}H]**6** [*max. stimulation of radioligand binding*][c] (n=3)[d]
Structure A: DIM or symmetric DIMs				
8	H			**0.368** ± 0.042 [*100 %*]
9 (PSB-16671)	5-F,7-F	H	H	**0.0415** ± 0.007 [*87 %*][d]
86 (PSB-16357)	4-F	H	H	**1.52** ± 0.19 [*56 %*]
87	4-Cl	H	H	**0.175** ± 0.016 [*94 %*]
88 (PSB-16105)	5-OCH_3	H	H	**0.103** ± 0.063 [*46 %*]
89 (PSB-15160)	5-F	H	H	**0.199** ± 0.049 [*125 %*][d]
90	5-Cl	H	H	**0.250** ± 0.080 [*90 %*][d]
91	5-Br	H	H	**0.0591** ± 0.0145 [*69 %*]
92 (PSB-16358)	6-F	H	H	**0.302** ± 0.059 [*57 %*][d]
93	6-Cl	H	H	(**43.7** ± 9.6)[b]
94 (PSB-16381)	7-F	H	H	**0.0618** ± 0.0136 [*153 %*]
95	5-F,6-Cl	H	H	**0.129** ± 0.009 [*36 %*]
96	4-F,5-F	H	H	**0.0836** ± 0.0167 [*67 %*]
97 (PSB-16586)	5-F,6-F	H	H	**0.0524** ± 0.0068 [*55 %*]
98	H	H	CH_3	(**14.0 ±** 4.2)[b]

99 (PSB-16359)	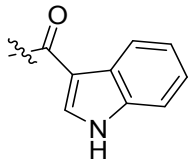	-	-	**1.93** ± 0.42 [*59 %*]
Structure B: unsymmetrically substituted diindolylmethane derivatives				
100	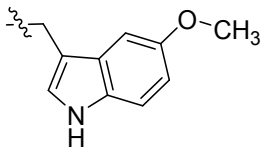	-	-	**0.495** ± 0.096 [*53 %*]
101(PSB-16244)	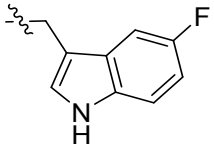	-	-	**0.276** ± 0.065 [*55 %*][d]
Structure C: Substitution of the methylene linker (C10)				
102	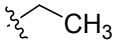	–		(**46.3** ± 14.9)[b]
103	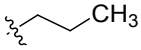	–		(**22.4** ± 9.60)[b]

[a]Affinities were determined in competition binding experiments using 2 nM [^{3}H]**6** and membrane preparations of CHO cells recombinantly expressing hGPR84. Screenings were performed at a concentration of 10 µM. [b]IC_{50} values (inhibition of radioligand binding). [c]Max. stimulation (%) of radioligand binding relative to the max. binding of [^{3}H]**6** in absence of test compound (DMSO-control (=100 %)). [d]n=4.

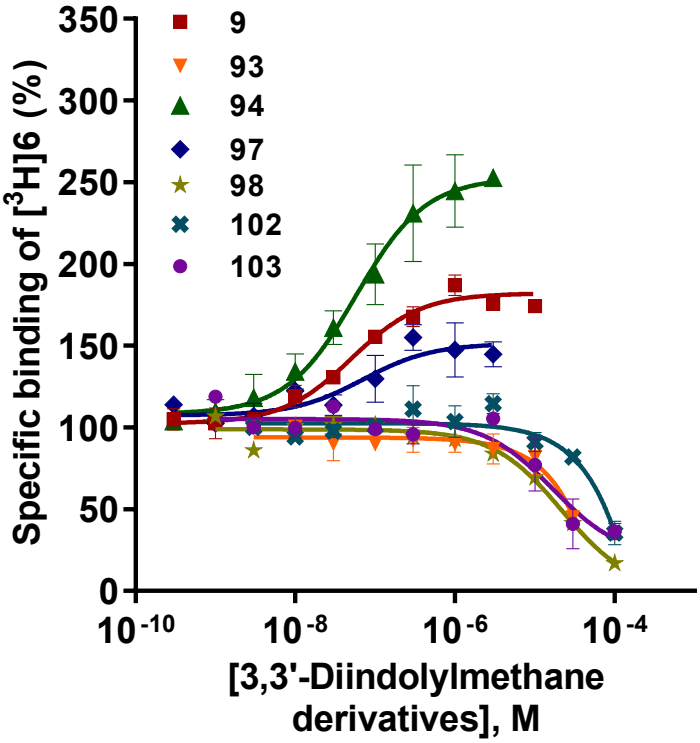

Figure 6. Competition binding experiments at membrane preparations of recombinant CHO cells expressing human GPR84. Allosteric modulation of radioligand binding by 3,3'-diindolylmethane derivatives. Data points represent means ± SEM from 3-7 independent experiments, each performed in duplicates. For EC_{50} and IC_{50} values (B) see Table 5.

There was a certain correlation of EC_{50} values determined in cAMP accumulation assays with EC_{50} values determined in radioligand binding studies ($R^2 = 0.433$, see Figure 7). For example, the most potent GPR84 agonist from this series, the tetrafluoro-DIM **9**, showed almost the same EC_{50} value in cAMP assays as in the binding study (41.3 nM, Table 1, as compared to 41.5 nM, Table 5).

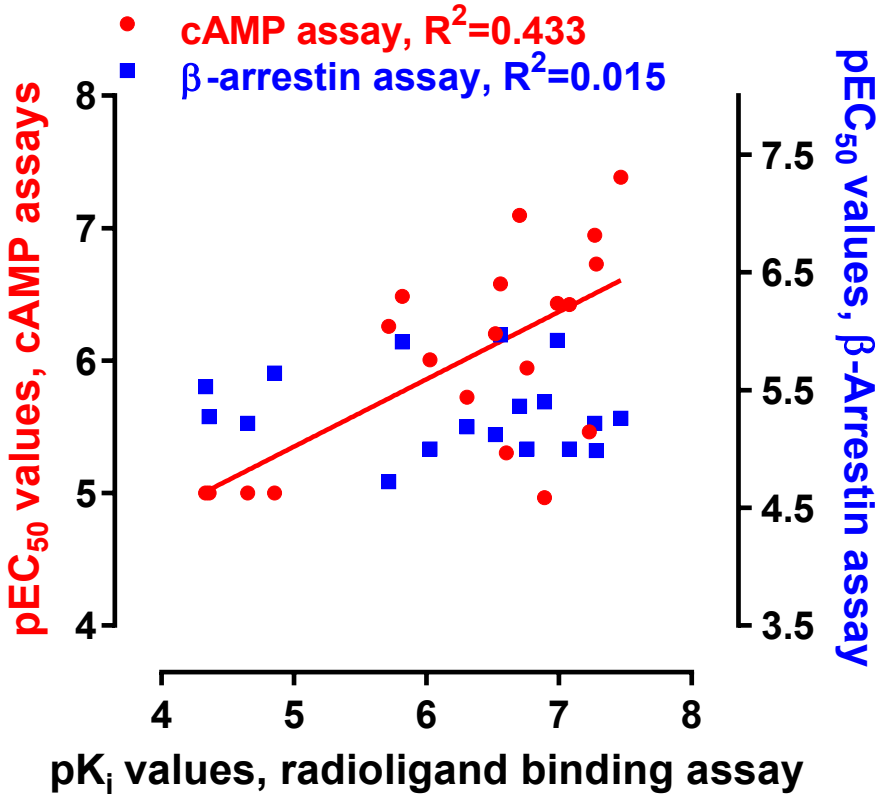

Figure 7. Correlation of pEC_{50} values of DIM derivatives determined in cAMP assays (●) or β-arrestin assays (■) with their respective pK_i values determined in radioligand binding assays. The same cell line (CHO-β-arrestin-human GPR84 cells) was used for all assays. R^2 was determined in a two-tailed Pearson test.

Most compounds displayed a difference of less than 6-fold in both assays. There were a few exceptions: 5,5'-dichloro-DIM (**90**, 20-fold), 5,5'-dibromo-DIM (**91**, 58-fold), 5,5'-difluoro-6,6'-dichloro-DIM (**95**, 84-fold), which were considerably more potent in the binding as compared to the cAMP assay. If those three outliers were excluded, the correlation was much better ($R^2 = 0.790$). In contrast, data from binding studies did not at all correlate with EC_{50} values determined in β-arrestin assays (see Figure 7). A few DIM derivatives and analogs, compounds **93**, **98**, **102** and **103**, which had previously been found to be inactive in cAMP assays, but observed to be weak

agonists in the β-arrestin assays at GPR84, were found to inhibit rather than increase radioligand binding (see Table 5 and Figure 6). These data underscore the complexity of the interactions of these ago-allosteric modulators with GPR84.

Molecular modeling studies

Data from radioligand binding studies represent an ideal basis for molecular modeling studies since they are derived from the direct interaction of the compounds with the receptor.

Homology model of the human GPR84.

In order to rationalize the binding modes of the known GPR84 agonists decanoic acid (**1**), embelin (**2**), 6-octylaminouracil (**3**) and its derivatives **6** and **7**, and their interactions with the human GPR84, a homology model of the receptor was generated. Among the different GPCR sequences determined by BLAST (Basic Local Alignment Search Tool) search against the Protein Data Bank (PDB), the human dopamine D3 receptor was selected,[43] which had been co-crystallized with eticlopride (PDB ID: 3PBL).[44] Although the amino acid sequence of the human GPR84 and the dopamine D3 receptor display a low degree of identity (24.6 %), the sequence alignment based on the transmembrane motifs both feature a large intracellular loop 3 (ICL3). This supported the selection of the human dopamine D3 receptor as a template for generating the homology model of the human GPR84. The sequence alignment between the human GPR84 and the human dopamine D3 receptor is shown in Figure S18. Previous attempts by Nikaido et al. to generate a homology model for the human GPR84 had been based on the crystal structure of the human β_2-adrenergic receptor whose X-ray structure was available at that time.[22] Recently, another homology model of the human GPR84 was generated by Tikhonova using a combination of structures of the human orexin receptor OX1 with the extracellular loop 2 (ECL2) of rhodopsin.[45] In the present study, we

selected the dopamine D3 receptor and aligned it using ClustalO to GPR84 with the transmembrane motifs as well as the loop regions, and manually adjusted it to improve the alignment. From 100 generated models, the presented homology model of the human GPR84 was selected based on the Discrete Optimized Protein Energy (DOPE) score included in Modeller9. Generation of the Ramachandran plot gave seven residues having Phi/Psi angles in the disallowed ranges, while the percentage of residues having Phi/Psi angles in the most favorable range was around 98 % confirming good stereochemical quality of the selected model (see Figure S19).[46,47] PROSA II profile analysis verified the sequence structure compatibility of the model with a Z-score of -2.52 (see Figure S20).[49]

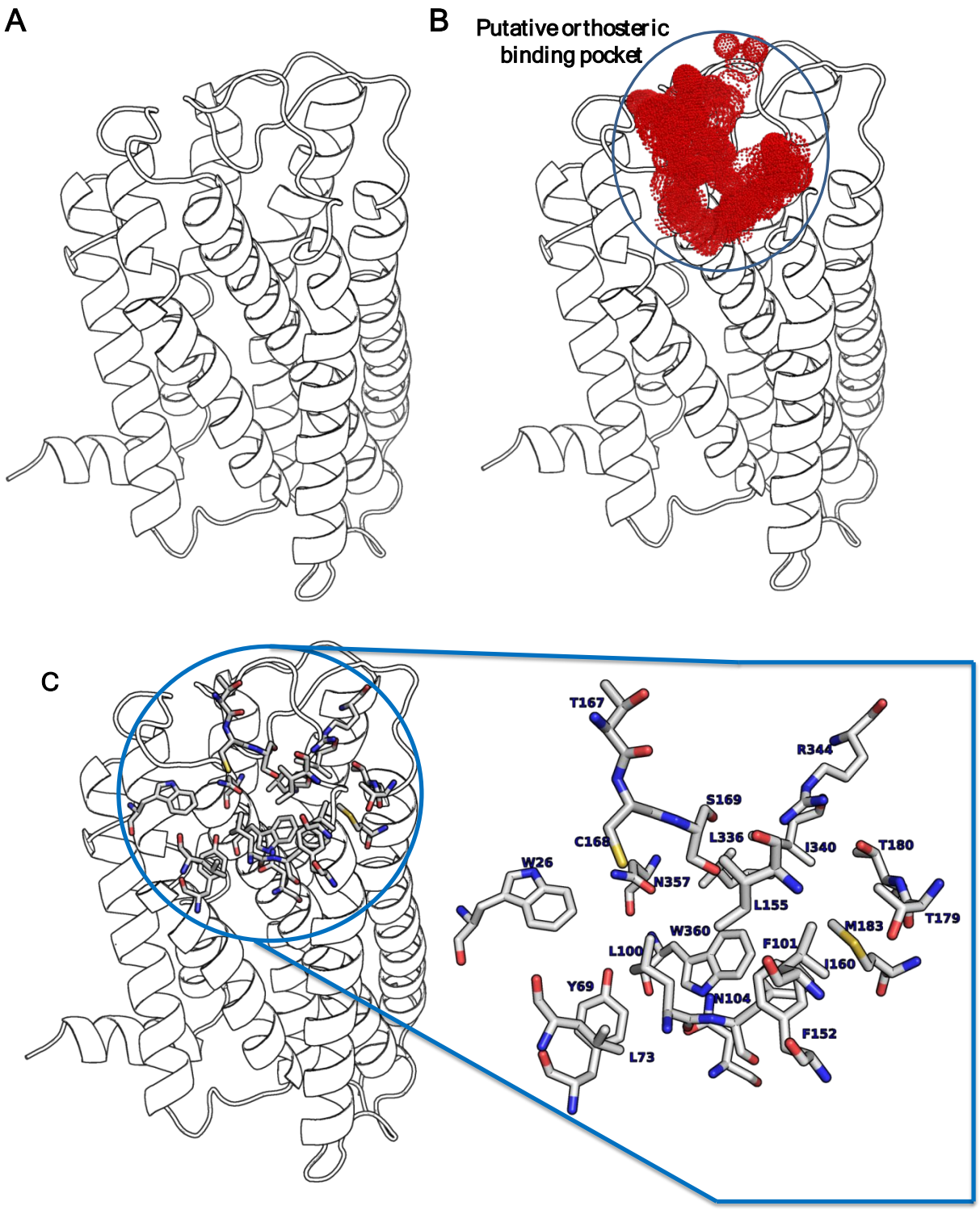

Figure 8. Homology model of the human GPR84. **A**. Homology model of the human GPR84 based on the human dopamine D3 receptor crystal structure (PDB ID: 3PBL). **B**. The putative orthosteric

binding site of the human GPR84 predicted using SiteFinder implemented in MOE is schematically indicated and depicted as red spheres. **C**. The important amino acid residues in the presumed orthosteric binding pocket are shown. Carbon atoms are colored in gray, oxygen atoms in red, nitrogen atoms in blue and sulfur atoms in yellow.

Due to the horizontal binding orientation of eticlopride in the human dopamine D3 receptor crystal structure used as a template, the putative orthosteric binding pocket of the generated human GPR84 model was partially closed. This was mainly due to the predicted conformation of the ECL2 that partially projected into the putative orthosteric binding site of the receptor model. Thus, the best model of the human GPR84 selected based on the DOPE score was further refined by using the loop modeler module implemented in Molecular Operating Environment (MOE 2014.09).[49] This led to the identification of the putative orthosteric binding site of the human GPR84 with a volume of 173 $Å^3$ using the SiteFinder module from MOE 2014.09. The important amino acids in the orthosteric binding site of the human GPR84 are shown in Figure 8. Interestingly, no positively charged residues as in the fatty acid receptors FFA1-3 (lArg185 and Arg258), or in the fatty acid receptor FFA4 (Arg99), were observed in the putative orthosteric binding site of GPR84. This shows that the binding site of the human GPR84 is very different from that of FFAR1-4.

Docking studies of the agonists. In order to rationalize the binding affinities of the agonists for GPR84 determined in radioligand binding studies, the binding modes of the potent uracil derivatives **3**, **6** and **7** were predicted using molecular docking studies. For comparison, the standard GPR84 agonists decanoic acid (**1**) and embelin (**2**) were docked into the binding site of the receptor. In an earlier mutagenesis study by Nikaido et al. based on their homology model of the human GPR84, the authors investigated the role of nine amino acids located in the putative orthosteric binding site of the receptor.[22] Among these, mutation of Leu100 (L100D), Phe101 (F101Y), Asn104 (N104Q) or Asn357 (N357D) resulted in a significant reduction or even a complete loss of the activity of the agonist decanoic acid. In the present docking study, we utilized the published mutagenesis data for selecting the putative binding poses of the selected agonists. The resulting proposed docking poses of **1-3**, **6** and **7** are shown in Figure 9.

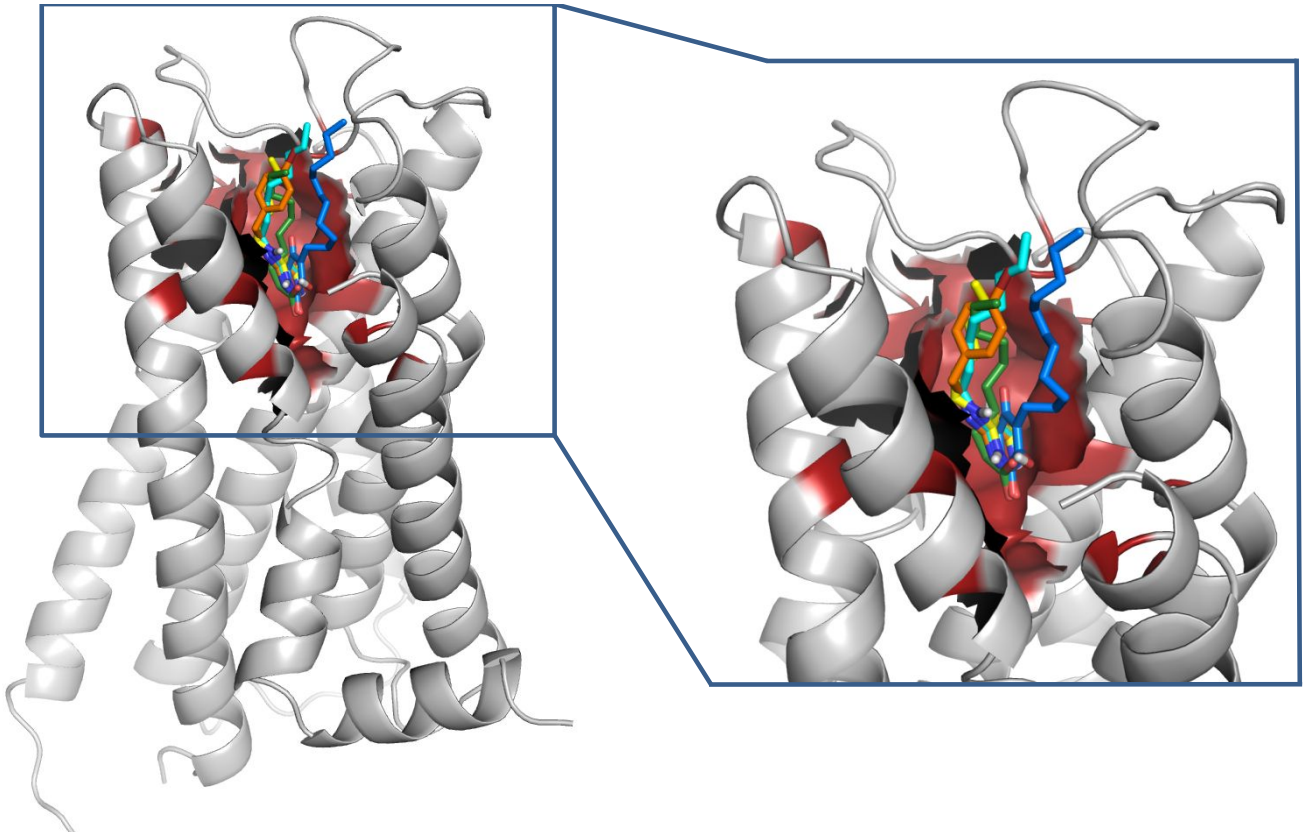

Figure 9. Docking studies of selected agonists at the human GPR84 model (based on the human dopamine D3 receptor crystal structure, PDB ID: 3PBL). The docked poses of decanoic acid (**1**, green), embelin (**2**, marine blue) and uracil derivatives **3** (cyan), **6** (yellow) and **7** (orange) in the orthosteric binding pocket (surface representation, colored maroon red) of the human GPR84 model are displayed in cartoon representation (gray).

Figure 10A depicts the amino acid residues in the putative binding site. The proposed interactions for the selected agonists **1**, **2**, and **6** are shown in Figures 10B-D, while those for compounds **3** and **7** are depicted in Supplementary Figure S29 A-B. The depicted amino acid residues in the binding pocket of GPR84 are predicted to be important for interactions with all of these lipid-like agonists. The compounds are proposed to be anchored inside the binding cleft by hydrogen bond interactions with Tyr69, Asn104, and Asn357. The carboxylate function of **1** likely forms interactions with Tyr69, Asn104, and Asn357. In embelin (**2**), the C1-keto group is presumed to form interactions with Tyr69 and Asn104, and the 2-hydroxy group likely forms interactions with Asn357. Similar interactions were observed for the uracil derivatives **3**, **6** and **7** in the model: the C2-carbonyl group is proposed to form interactions with Tyr69 and Asn104, and the N1-H to interact with Asn357. The space between the C4-carbonyl group in uracil derivatives and the nearby amino acids in the binding pocket suggests a water-mediated interaction. Similarly, the OH-group at position 2 of embelin might be deprotonated and form interactions with Asn357 in the binding site. Furthermore, in uracil derivatives **3**, **6** and **7**, the 6-NH group is proposed to form a strong interaction with Asn357, and the N3-H possibly forms interactions with Asn104 located at a distance of ~3 Å. These two interactions could not be observed for the GPR84 agonists decanoic acid (**1**) and embelin (**2**) in our model. This could explain why higher binding affinities are obtained for the uracil derivatives (e.g. **3**, K_i 0.626 nM) in comparison to **1** (K_i 1780 nM) and **2** (K_i 23.6 nM). The residues

Leu100, Phe101, and Trp360 form a hydrophobic subpocket, which likely interacts with the lipophilic GPR84 agonists. Possibly, this hydrophobic interaction is stronger for embelin (**2**) and the uracil derivatives as compared to the weakly potent decanoic acid (**1**). The findings of a hydrophobic interaction of Leu100 and Phe101 with **1** are in agreement with the experimental mutagenesis data obtained by Nikaido et al. because the mutants L100D, L100N and F101Y resulted in a very weak activity possibly due to impairment of these hydrophobic interactions.[22] Furthermore, the mutation of N104Q might break the hydrogen bond interaction between the carboxylate group of **1** and Asn104. Interestingly, another mutant, N357D, resulted in an almost complete loss of activity of agonist **1**, possibly due to breaking the hydrogen bond interaction between the carboxylate and Asn357. The previously published homology model of the human GPR84 that was based on the β_2-adrenergic receptor, focused on positively charged residues that could anchor the carboxylate function of free fatty acids in the receptor.[45] However, a negative charge is not required for high GPR84 affinity. Therefore, the current study focused on the published mutagenesis data as well as the structure-activity relationships observed in binding studies, and the proposed model is well in agreement with those data. The long alkyl chains plausibly bind within the cleft that is largely formed by the hydrophobic amino acids Leu84, Leu100, Thr167, Cys168, Phe170, Leu336, Ile340, and Met353. The alkyl chain plays a major role in anchoring the molecules in order to form key interactions with the residues Tyr69, Asn104, and Asn357 in the binding site. For example, we found in the series of uracil derivatives that the binding affinity of the alkyl chain length of five carbon atoms (**28**, K_i 91.0 nM) is significantly increased with an additional methylene unit in **6** (K_i 2.98 nM). Further extension of the alkyl chain length in derivatives **3**, and **29-31** led to a further, moderate increase in binding affinity (see Table 3). Moreover, introducing an aromatic residue into the alkyl chain in **6** results in effective occupation of the cleft forming strong hydrophobic interactions with the amino acids in the binding site,

resulting in a K_i value of 0.317 nM for agonist **7**. The large bromo substituent in **7** may further improve hydrophobic interactions with the amino acid residues of Leu84, Thr167, Cys168, and Phe170. This was confirmed by radioligand binding data showing a reduction in affinity in the following rank order: 4-Br (**7**, K_i 0.317 nM) ≥ 4-Cl (**37**, K_i 0.650 nM) > 4-F (**36**, K_i 11.4 nM).

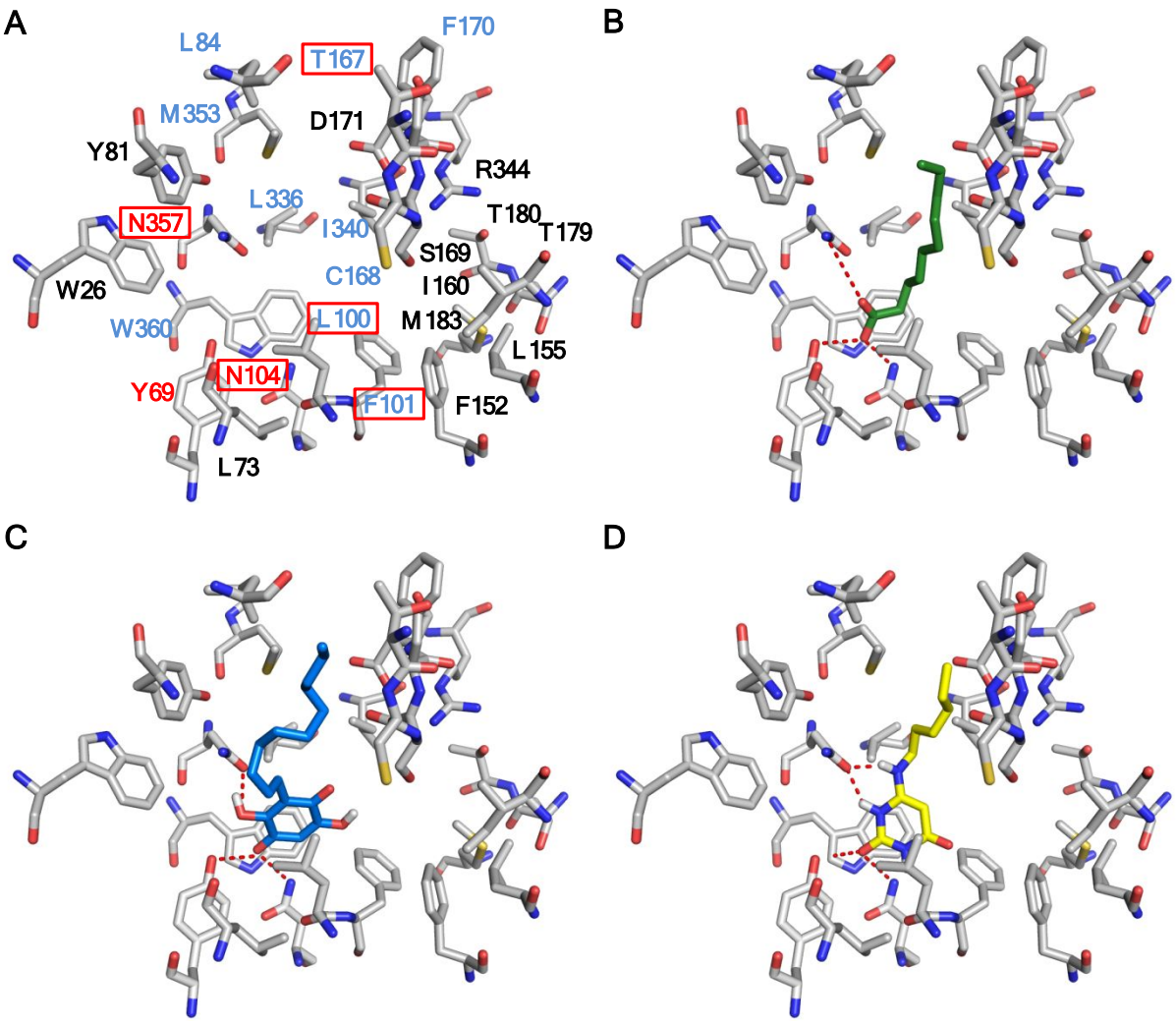

Figure 10. Binding site residues of the human GPR84 model (based on the human dopamine D3 receptor crystal structure, PDB ID: 3PBL) and putative binding modes of agonists. **A**. Important residues in the binding pocket are shown. The amino acid residues forming hydrogen bond interactions are labeled in red color, hydrophobic interactions in blue and the mutants published by

Nikaido et al. are highlighted by red boxes.[22]Binding poses of agonists in the putative orthosteric binding site: **B**. decanoic acid (**1**, green); **C**. embelin (**2**, marine blue); **D.** 6-hexylaminouracil (**6**, yellow);Red dotted lines indicate hydrogen bond interactions (for further color code see Figure 9).

The recent study by Mahmud et al. proposed a different binding site and mode of interaction for agonists **1**, **2** and **4** on the basis of a hybrid homology model of the human GPR84 generated using the OX1 receptor and the rhodopsin crystal structures.[25] The authors proposed that the amino acid residue Arg172 in the ECL2 of GPR84 is oriented towards the proposed orthosteric binding site and possibly coordinates the agonists **1**, **2** and **4**. To confirm this hypothesis, an R172A mutant was generated, and the above mentioned agonists were examined using [^{35}S]GTPγS binding studies.[25] In that mutant, the affinity of the agonists was lost, but it was also lost for another mutant, R172K, in which Arg172 was replaced by another positively charged residue, a lysine. However, this homologous exchange did not lead to a retention or salvage, not even partially, of the agonists' potency. Based on the published mutagenesis results, and according to the visualization of our generated homology model, and the performed docking studies, Arg172 does not appear to be directly interacting with the orthosteric agonists. Our current hypothesis is that Arg172 might contribute indirectly to agonist-receptor interaction by inducing a certain conformation in the ECL2 or by disturbing the interaction of Thr167 with agonists.

Labeling of GPR84 in native cells and tissues. Finally, we utilized the new radiotracer as a tool for detecting and quantifying GPR84 on the protein level in cells and tissues. It is expected to be advantageous, since antibodies for membrane proteins are often not selective. Therefore, we performed radioligand binding studies in different cell and organ preparations. High specific

binding of [^{3}H]**6** was detected in HepG2 (human hepatocarcinoma) cells, Jurkat (human T-lymphocyte) cells, HEK293 (human embryonic kidney) cells and native human T-lymphocytes, while in MCA-RH7777 (rat buffalo hepatoma) cells and C6 glioma (rat glioblastoma) cells no specific binding was detectable. Moreover, we could observe specific [^{3}H]**6** binding in liver tissues (calf, mouse, rat) as well as in rat brain cortex and striatum (Figure 11). Next, we performed competition experiments with selected tissues and cell lines in order to determine IC_{50} values for 6-hexylaminouracil (**6**) and 6-(*p*-bromophenylethylamino)uracil (**7**) (see Figure S30). The GPR84 agonist **6** displayed higher IC_{50} values in all tested tissues and cell lines (8- to 76-fold) compared to the IC_{50}/K_i value determined in CHO-human GPR84 cells (Table S3). This might be due to the presence of endogenous GPR84 agonists in the preparations. Although MCFAs were shown to activate GPR84, another, perhaps significantly more potent endogenous agonist might exist whose discovery is still awaited. Interestingly, in all tested human tissues and cell lines, **7** showed higher affinity than **6**, while in rodent tissues the opposite was true. Here, **6** displayed 2 to 5-fold higher affinity than **7** indicating species differences (Table S3 and Figure S30).

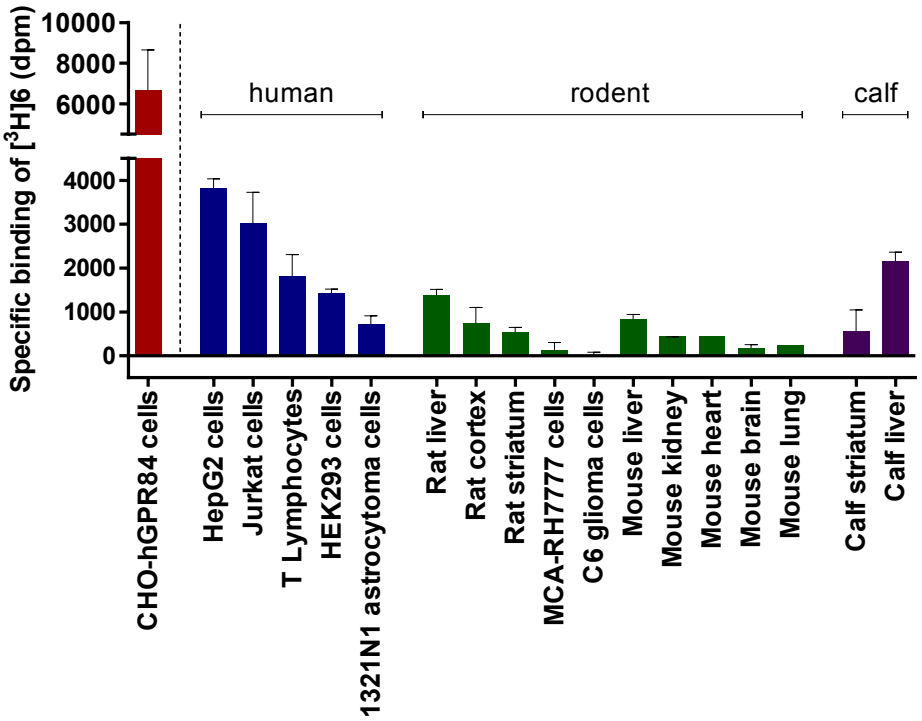

Figure 11. Specific binding of [^{3}H]**6** to membrane preparations of various native tissues and cell lines. The experiments were performed at 25°C using 10 nM [^{3}H]**6** and 100 µg protein/vial, except for Jurkat cells and T-lymphocytes: 25 µg protein/vial; HepG2 cell: 2 nM RL. Agonist **7** was used for the determination of non-specific binding. Data points represent means ± SEM from 3-5 independent experiments, each performed in duplicates. At low GPR84 expression levels the percentage of non-specific binding is relatively high, and the data is consequently less accurate.

Conclusions

In conclusion, we developed the first GPR84 agonist radioligand [^{3}H]**6** for studying the binding affinities of receptor ligands. [^{3}H]**6** was found to exhibit high affinity for the human GPR84 along with a low degree of nonspecific binding. Its binding was discovered to be modulated by ions, Mg^{2+} increasing, Na^+ reducing its binding affinity. As expected, lipid-like GPR84 agonists inhibited [^{3}H]**6** binding while DIM and the majority of its derivatives induced an increase in [^{3}H]**6** binding, which provides the ultimate evidence for their positive allosteric modulation of the receptor. For 6-(ar)alkylamino-substituted uracil derivatives, the rank order of the determined affinities correlated mostly with EC_{50} values obtained in cAMP assays, while only weak correlation was seen with EC_{50} values determined in β-arrestin assays. A series of new lipid-like agonists (**62-68**, **73-77**, **79-85**) was synthesized and evaluated in binding studies to analyze their SARs. Finally, we generated a homology model of the human GPR84, performed docking studies of selected agonists, and rationalized the observed structure-activity relationships. The predicted binding modes and interactions with the amino acids in the binding site including Leu100, Phe101, Asn104, and Asn357, were well in agreement with previously reported mutagenesis data. Moreover, we could show that [^{3}H]**6** is useful to label human GPR84 in native tissues. The developed GPR84 agonist radioligand represents a powerful pharmacological tool to further explore this yet poorly characterized orphan receptor.

Experimental section

General Methods. All commercially available reagents were used as purchased (Acros, Alfa Aesar, Sigma-Aldrich, abcr or TCI). Solvents were used without additional purification or drying except for dichloromethane, which was distilled over calcium hydride. Thin layer chromatography (TLC) using aluminum sheets with silica gel 60 F254 monitored the reactions (Merck). Column

chromatography was performed with silica gel 0.060-0.200 mm, pore diameter ca. 6 nm. All synthesized compounds were finally dried in vacuum at 8-12 Pa (0.08-0.12 mbar) using a sliding vane rotary vacuum pump (Vacuubrand GmbH). ^{1}H- and ^{13}C NMR data were collected on a Bruker Avance 500 MHz NMR spectrometer at 500 MHz (^{1}H), or 126 MHz (^{13}C), respectively. If indicated, NMR data were collected on a Bruker Ascend 600 MHz NMR spectrometer at 600 MHz (^{1}H), or 151 MHz (^{13}C), respectively. DMSO-d_6 was employed as a solvent at 303 K, unless otherwise noted. Chemical shifts are reported in parts per million (ppm) relative to the deuterated solvent; that is, DMSO, δ ^{1}H: 2.49 ppm; ^{13}C: 39.7 ppm. Coupling constants *J* are given in Hertz and spin multiplicities are given as s (singlet), d (doublet), t (triplet), q (quartet), sext. (sextet), m (multiplet), br (broad). The purities of isolated products were determined by ESI-mass spectra obtained on an LCMS instrument (Applied Biosystems API 2000 LCMS/MS, HPLC Agilent 1100) using the following procedure: the compounds were dissolved at a concentration of 1.0 mg/mL in acetonitrile containing 2 mM ammonium acetate. Then, 10 μL of the sample were injected into an HPLC column (Macherey-Nagel Nucleodur® 3 μ C18, 50 x 2.00 mm). Elution was performed with a gradient of water/acetonitrile (containing 2 mM ammonium acetate) from 90:10 to 0:100 for 20 min at a flow rate of 300 μL/min, starting the gradient after 10 min. UV absorption was detected from 200 to 950 nm using a diode array detector (DAD). Purity of all compounds was determined at 254 nm. Compounds **1**, **2**, and **16-27** were commercially available. Compounds **12** and **13** were synthesized according to the reported procedure.[50] The syntheses of compounds **3**,[24] **4**,[28] **5**,[29] 6,[24] **7**,[24] **28-60**,[24] and **8**,[26] **9**,[26] **86-103**[26] were previously described. Purities of all products were determined by HPLC-UV-MS and proven to be >95%.

Synthesis of (*E*)-6-(hex-2-en-1-ylamino)pyrimidine-2,4(1*H*,3*H*)-dione (15)

To the solution of **14** (1.0 g, 6.8 mmol) in 1-butanol (20 ml) was added (*E*)-hex-2-en-1-amine[51] (**13**, 2.03 g, 20.5 mmol, 3 equiv.). The resulting solution was heated up to 125 ^{o}C and stirred under reflux for 12 h. After cooling to room temperature, 1-butanol was evaporated under the reduced pressure. The resulting residue was washed with cold 1-butanol (10 ml) and diethyl ether (10 ml), and the solid was dried under vacuum for 6 h.

Synthesis of 6-(hexylamino)pyrimidine-2,4(1*H*,3*H*)-dione (6)

Procedure A: To the solution of compound **15** (0.035 g, 0.167 mmol) in MeOH:THF (1:1), Pd/C (10%) (0.006 g) was added and the mixture was thrice evacuated and flushed with hydrogen (H_2). The reaction was performed at 25 psi (1.7 bar) for 2 h at room temperature. After completion of the reaction, the mixture was filtered through Celite, washed with MeOH:THF (1:1) mixture (20 mL) and evaporated to get the compound **6**.

Procedure B: To the solution of compound **15** (0.040 g, 0.191 mmol) in DMF:THF (1:1), Pd/C (10%) (0.016 g) was added and the mixture was thrice evacuated and flushed with hydrogen (H2). The reaction was performed at 35 psi (2.4 bar) for 2 hour at room temperature. After completion of the reaction, the mixture was filtered through Celite, washed with DMF:THF (1:1) mixture (20 mL) and evaporated to remove THF. The compound in DMF was treated with water (10 ml) and the resulting solid was filtered and dried under vacuum to produce **6**, which characterized in a previous report.[24]

Synthesis of 4, 62-68 and 73-76

To the solution of 2-mercaptopyrimidine-4,6-diol (**61**, 1.0 mmol), 2-mercaptopyrimidin-4-ol (**69**, 1.0 mmol), 2-mercapto-6-methylpyrimidin-4-ol (**70**, 1.0 mmol), 2-mercapto-6-propylpyrimidin-4-

ol (**71**, 1.0 mmol), or 2-mercaptopyrimidine-4-carboxylic acid (**72**, 1.0 mmol) and aryl(alkyl)bromides (2 mmol) in methanol, K_2CO_3 (3.0 mmol) was added The resulting solution was refluxed under a nitrogen atmosphere for 12 h. The reaction mixture was allowed to cool to room temperature, and methanol was evaporated under reduced pressure to the dryness. The residue was dissolved in ethyl acetate (100 mL) and washed with water (50 mL). The organic layer was dried over $MgSO_4$, filtered and concentrated under reduced pressure to afford a crude product, which was purified by silica gel column chromatography (DCM:MeOH = 99:5) to afford the desired products **4, 62-68 and 73-76**.

Synthesis of 77

To the solution of **76** (0.5 mmol) in methanol (20 mL), 2 N NaOH was added (1 mL) and resulting solution was refluxed for 1 h. The reaction mixture was allowed to cool to room temperature, and methanol was evaporated under reduced pressure to the dryness. The residue was dissolved in water (10 mL) and acidified with 2 N HCl (20 mL). The resulting precipitate was filtered, washed with water (20 mL) and dried under open air for 24 h.

Synthesis of 79 and 80

To the solution of **78** (10 mmol) in appropriated alcohol (20 mL), concentrated H_2SO_4 (0.1 mmol) was added under ice cooling condition. The solution was warmed up and refluxed for 12 h. The reaction mixture was allowed to cool to room temperature, and ethyl acetate (100 mL) and water (100 mL) were added. The organic layer was separated, dried over $MgSO_4$, filtered and concentrated to afford a crude residue, which was purified by silica gel column chromatography (DCM:MeOH = 98:2) to afford the desired product **79** or **80**.

Synthesis of 81-85

To the solution of **78** (10 mmol), appropriate amine (10.5 mmol), HATU (10.5 mmol) in DMF (15 mL), triethylamine (25 mmol) was added slowly. The resulting solution was stirred at room temperature for 12 h. The mixture was poured onto ice water, separated with ethylacetate (3 x 50 mL). The combined organic layers was washed with brine solution, dried over MgSO4, filtered and concentrated to afford a crude residue, which was purified by silica gel column chromatography (DCM:MeOH = 95:5) to afford the desired product **81-85**.

2-(Hexylthio)-6-hydroxypyrimidin-4(3*H*)-one (4)

Compound **6** was synthesized from the reaction of 6-hydroxy-2-mercaptopyrimidin-4(3*H*)-one (**61**, 1.0 mmol) with 1-bromohexane (2.0 mmol) in the presence of K_2CO_3 (3.0 mmol) in methanol. Yield 37%: colorless solid; ^{1}H NMR (500 MHz, DMSO-d_6) δ 11.65 (s, 2H), 5.10 (s, 1H), 3.07 (t, J = 7.2 Hz, 2H), 1.60 (p, J = 7.3 Hz, 2H), 1.48 – 1.18 (m, 6H), 1.10 – 0.47 (m, 3H). ^{13}C NMR (126 MHz, DMSO-d_6) δ 85.70, 30.85, 29.66, 28.81, 27.90, 22.11, 13.98. LC-MS (m/z): positive mode 229 $[M+H]^{1+}$; Purity by HPLC UV (254 nm)-ESI-MS: 98.0%.

(*E*)-6-(Hex-2-en-1-ylamino)pyrimidine-2,4(1*H*,3*H*)-dione (15)

Yield: 91%; Pale yellow solid; ^{1}H NMR (500 MHz, DMSO-d_6) δ 10.10 (s, 1H), 9.32 (s, 1H), 6.19 (t, J = 5.7 Hz, 1H), 5.70 – 5.50 (m, 1H), 5.50 – 5.24 (m, 1H), 4.39 (s, 1H), 3.59 (t, J = 5.8 Hz, 2H), 1.98 (q, J = 6.9 Hz, 2H), 1.35-1.33 (m, J = 7.3 Hz, 2H), 0.87 (m, 3H). ^{13}Capt NMR (126 MHz, DMSO-d_6) δ 164.30, 154.06, 150.91, 132.77, 125.60, 73.12, 43.25, 33.76, 21.90, 13.58. LC-MS (m/z): positive mode 210 $[M+H]^{1+}$; Purity by HPLC UV (254 nm)-ESI-MS: 98.5%.

6-Hydroxy-2-((3-phenylpropyl)thio)pyrimidin-4(3*H*)-one (62)

Compound **62** was synthesized from the reaction of **61** (1.0 mmol) with 1-bromo-3-phenylpropane (2.0 mmol) in the presence of K_2CO_3 (3.0 mmol) in methanol. Yield: 56%; colorless solid; ^{1}H

NMR (500 MHz, DMSO-d_6) δ 11.73 (s, 2H), 7.29 (t, J = 7.7 Hz, 2H), 7.20 (dd, J = 17.9, 7.7 Hz, 3H), 3.10 (t, J = 7.1 Hz, 2H), 2.70 (t, J = 7.7 Hz, 2H), 1.95 (p, J = 7.4 Hz, 2H). ^{13}C NMR (126 MHz, DMSO-d_6) δ 141.28, 128.52, 128.45, 126.06, 85.78, 34.22, 30.53, 29.37. LC-MS (m/z): positive mode 263 $[M+H]^{1+}$; Purity by HPLC UV (254 nm)-ESI-MS: 98.9%.

6-Hydroxy-2-((3-phenylbutyl)thio)pyrimidin-4(3*H*)-one (63)

Compound **63** was synthesized from the reaction of **61** (1.0 mmol) with 1-bromo-4-phenylbutane (2.0 mmol) in the presence of K_2CO_3 (3.0 mmol) in methanol. Yield: 62%; colorless solid; ^{1}H NMR (500 MHz, DMSO-d_6) δ 11.61 (s, 2H), 7.38 – 7.22 (m, 2H), 7.22 – 6.99 (m, 3H), 5.11 (s, 1H), 3.11 (t, J = 6.6 Hz, 2H), 2.59 (t, J = 7.1 Hz, 2H), 1.65 (pt, J = 5.0, 2.9 Hz, 4H). ^{13}C NMR (126 MHz, DMSO-d_6) δ 142.02, 128.37, 128.36, 125.81, 85.70, 34.67, 30.05, 29.41, 28.53. LC-MS (m/z): positive mode 277 $[M+H]^{1+}$; Purity by HPLC UV (254 nm)-ESI-MS: 97.3%.

2-((4-Fluorophenethyl)thio)-6-hydroxypyrimidin-4(3*H*)-one (64)

Compound **64** was synthesized from the reaction of **61** (1.0 mmol) with 4-fluorophenethyl bromide (2.0 mmol) in the presence of K_2CO_3 (3.0 mmol) in methanol. Yield: 72%; Colorless solid; ^{1}H NMR (500 MHz, DMSO-d$_6$) δ 7.50 – 7.22 (m, 2H), 7.22 – 6.87 (m, 2H), 5.14 (s, 1H), 3.30 (d, J = 6.1 Hz, 2H), 2.92 (dd, J = 8.5, 6.7 Hz, 2H). ^{13}C NMR (126 MHz, DMSO-d$_6$) δ 160.13, 136.25, 136.22, 130.65, 130.59, 115.21, 115.04, 85.77, 34.03, 31.03. LC-MS (m/z): positive mode 267 $[M+H]^{1+}$; Purity by HPLC UV (254 nm)-ESI-MS: 95.7%.

2-((4-Clorophenethyl)thio)-6-hydroxypyrimidin-4(3*H*)-one (65)

Compound **65** was synthesized from the reaction of **61** (1.0 mmol) with 4-chlorophenethyl bromide (2.0 mmol) in the presence of K_2CO_3 (3.0 mmol) in methanol. Yield: 69%; Colorless solid; ^{1}H NMR (500 MHz, DMSO-d_6) δ 7.39 – 7.33 (m, 2H), 7.33 – 7.27 (m, 2H), 5.14 14 (s, 1H), 3.30 (s, 2H merged with H_2O peak), 2.93 (dd, J = 8.5, 6.7 Hz, 2H). ^{13}C NMR (126 MHz, DMSO-d_6) δ

139.09, 131.13, 130.70, 128.36, 85.76, 34.13, 30.77. LC-MS (m/z): positive mode 283 $[M+H]^{1+}$; Purity by HPLC UV (254 nm)-ESI-MS: 98.7%.

2-((4-Bromophenethyl)thio)-6-hydroxypyrimidin-4(3*H*)-one (66)

Compound **66** was synthesized from the reaction of **61** (1.0 mmol) with 4-bromophenethyl bromide (2.0 mmol) in the presence of K_2CO_3 (3.0 mmol) in methanol. Yield: 57%; Colorless solid; ^{1}H NMR (500 MHz, DMSO-d_6) δ 7.68 – 7.31 (m, 2H), 7.39 – 6.97 (m, 2H), 5.14 (s, 1H), 3.32 (s, 2H), 2.92 (dd, J = 8.5, 6.6 Hz, 2H). ^{13}C NMR (126 MHz, DMSO-d_6) δ 139.51, 131.29, 131.10, 119.58, 85.76, 34.18, 30.70. LC-MS (m/z): positive mode 328 $[M+H]^{1+}$; Purity by HPLC UV (254 nm)-ESI-MS: 96.9%.

2-((4-Methylphenethyl)thio)-6-hydroxypyrimidin-4(3*H*)-one (67)

Compound **67** was synthesized from the reaction of **61** (1.0 mmol) with 4-methylphenethyl bromide (2.0 mmol) in the presence of K_2CO_3 (3.0 mmol) in methanol. Yield: 77%; Colorless solid; ^{1}H NMR (500 MHz, DMSO-d_6) δ 7.16 (d, J = 8.1 Hz, 2H), 7.10 (d, J = 7.7 Hz, 2H), 5.13 (s, 1H), 3.35 – 3.29 (m, 3H), 2.88 (dd, J = 8.6, 6.7 Hz, 2H). ^{13}C NMR (126 MHz, DMSO-d_6) δ 167.30, 162.96, 136.98, 135.46, 129.03, 128.63, 85.76, 45.92, 34.43. LC-MS (m/z): positive mode 263 $[M+H]^{1+}$; Purity by HPLC UV (254 nm)-ESI-MS: 97.0%.

6-Hydroxy-2-((4-(trifluoromethyl)phenethyl)thio)pyrimidin-4(3*H*)-one (68)

Compound **68** was synthesized from the reaction of **61** (1.0 mmol) with 4-trifluoromethylphenethyl bromide (2.0 mmol) in the presence of K_2CO_3 (3.0 mmol) in methanol. Yield: 64%; Colorless solid; ^{1}H NMR (500 MHz, DMSO-d_6) δ 7.66 (d, J = 8.0 Hz, 2H), 7.52 (d, J = 7.9 Hz, 2H), 5.15 (s, 1H9; 3.36 (dd, J = 8.5, 6.6 Hz, 4H), 3.05 (s, 2H). ^{13}C NMR (126 MHz, DMSO-d_6) δ 154.53, 144.98, 129.67, 85.77, 34.59, 30.50. LC-MS (m/z): positive mode 317 $[M+H]^{1+}$; Purity by HPLC UV (254 nm)-ESI-MS: 95.6%.

2-(Hexylthio)pyrimidin-4-ol (73)[51]

Compound **73** was synthesized from the reaction of 4-hydroxy-pyrimidine-2(1H)-thione (**69**, 1.0 mmol) with 1-bromohexane (2.0 mmol) in the presence of K_2CO_3 (3.0 mmol) in methanol. The compound was characterized in a previous report. LC-MS (m/z): positive mode 213 $[M+H]^{1+}$; Purity by HPLC UV (254 nm)-ESI-MS: 96.6%.

2-(Hexylthio)-6-methylpyrimidin-4-ol (74)[52]

Compound **74** was synthesized from the reaction of 4-hydroxy-6-methylpyrimidine-2(1H)-thione (**70**, 1.0 mmol) with 1-bromohexane (2.0 mmol) in the presence of K_2CO_3 (3.0 mmol) in methanol. The compound was characterized in a previous report. LC-MS (m/z): positive mode 227 $[M+H]^{1+}$; Purity by HPLC UV (254 nm)-ESI-MS: 97.3%.

2-(Hexylthio)-6-propylpyrimidin-4-ol (75)

Compound **75** was synthesized from the reaction of 4-hydroxy-6-propylpyrimidine-2(1H)-thione (**71**, 1.0 mmol) with 1-bromohexane (2.0 mmol) in the presence of K_2CO_3 (3.0 mmol) in methanol. Yield 61%: Pale yellow solid; ^{1}H NMR (500 MHz, DMSO-d_6) δ 12.41 (s, 1H), 5.91 (s, 1H), 3.10 (t, J = 7.3 Hz, 2H), 2.39 (t, J = 7.4 Hz, 2H), 1.63 (ddt, J = 14.9, 10.8, 7.1 Hz, 4H), 1.41 – 1.25 (m, 5H), 0.88 (dt, J = 11.3, 7.2 Hz, 5H). ^{13}C NMR (126 MHz, DMSO-d_6) δ 168.22, 167.27, 164.07, 106.81, 30.82, 29.67, 29.01, 27.89, 22.05, 20.64, 13.96, 13.55. LC-MS (m/z): positive mode 255 $[M+H]^{1+}$; Purity by HPLC UV (254 nm)-ESI-MS: 97.7%.

Methyl 2-(hexylthio)-6-hydroxypyrimidine-4-carboxylate (76)[53]

Compound **76** was synthesized from the reaction of 6-hydroxy-2-thioxo-2,3-dihydropyrimidine-4-carboxylic acid (**72**, 1.0 mmol) with 1-bromohexane (2.0 mmol) in the presence of K_2CO_3 (3.0 mmol) in methanol. The compound was characterized in a previous report. LC-MS (m/z): positive mode 271 $[M+H]^{1+}$; Purity by HPLC UV (254 nm)-ESI-MS: 99.0%.

2-(Hexylthio)-6-hydroxypyrimidine-4-carboxylic acid (77)[54]

Compound **77** was synthesized by reaction of **76** with 2 N NaOH. The compound was characterized in a previous report. LC-MS (m/z): positive mode 257 $[M+H]^{1+}$; Purity by HPLC UV (254 nm)-ESI-MS: 98.2%.

Butyl 2,6-dioxo-1,2,3,6-tetrahydropyrimidine-4-carboxylate (79)

Compound **79** was synthesized from the reaction of orotic acid (**78**, 10 mmol) and butanol (20 ml) in the presence of concentrated H_2SO_4 (0.1 mmol). Yield: 64%; Brown solid; ^{1}H NMR (500 MHz, DMSO-d_6) δ 11.35 (s, 1H), 11.09 (s, 1H), 6.03 (s, 1H), 4.25 (t, J = 6.5 Hz, 2H), 1.75 – 1.53 (m, 2H), 1.53 – 1.19 (m, 2H), 0.90 (t, J = 7.4 Hz, 3H, -CH_3). ^{13}C NMR (126 MHz, DMSO-d_6) δ 163.89, 160.44, 150.94, 141.63, 103.66, 66.38, 29.91, 18.65, 13.65. LC-MS (m/z): positive mode 213 $[M+H]^{1+}$; Purity by HPLC UV (254 nm)-ESI-MS: 95.5%.

Hexyl 2,6-dioxo-1,2,3,6-tetrahydropyrimidine-4-carboxylate (80)

Compound **80** was synthesized from the reaction of orotic acid (**78**, 10 mmol) and hexanol (20 ml) in the presence of concentrated H_2SO_4 (0.1 mmol). Yield: 73%; Brown solid; ^{1}H NMR (500 MHz, DMSO-d_6) δ 11.35 (s, 1H), 11.09 (s, 1H), 6.02 (s, 1H), 4.24 (t, J = 6.5 Hz, 2H), 1.85 – 1.58 (m, 2H), 1.45 – 1.07 (m, 6H), 1.05 – 0.64 (m, 3H). ^{13}C NMR (126 MHz, DMSO-d_6) δ 63.87, 160.43, 150.93, 141.62, 103.64, 66.66, 30.94, 27.81, 25.03, 22.08, 13.98. LC-MS (m/z): positive mode 241 $[M+H]^{1+}$; Purity by HPLC UV (254 nm)-ESI-MS: 96.0%.

2,6-Dioxo-*N*-(3-phenylpropyl)-1,2,3,6-tetrahydropyrimidine-4-carboxamide (81)

Compound **81** was synthesized from the reaction of orotic acid (**78**, 10 mmol) with 3-phenylpropylamine (10 mmol) in the presence of HATU (10.5 mmol) and TEA (25 mmol) in DMF. Yield: 68%; Brown solid; ^{1}H NMR (500 MHz, DMSO-d_6) δ 11.18 (s, 1H), 10.54 (s, 1H), 8.77 (t, J = 5.6 Hz, 1H), 7.30 – 7.24 (m, 2H), 7.24 – 7.19 (m, 2H), 7.19 – 7.13 (m, 1H), 5.99 (s, 1H), 3.20 (td, J = 7.0, 5.5 Hz, 2H), 2.74 – 2.54 (m, 2H), 1.78 (tt, J = 7.6, 6.5 Hz, 2H). ^{13}C NMR (126 MHz,

DMSO-d_6) δ 164.36, 160.23, 145.59, 141.67, 141.67, 128.45, 125.93, 125.93, 99.73, 32.58, 30.40. LC-MS (m/z): positive mode 274 $[M+H]^{1+}$; Purity by HPLC UV (254 nm)-ESI-MS: 97.5%.

2,6-Dioxo-*N*-pentyl-1,2,3,6-tetrahydropyrimidine-4-carboxamide (82)

Compound **82** was synthesized from the reaction of orotic acid (**78**, 10 mmol) with pentylamine (10 mmol) in the presence of HATU (10.5 mmol) and TEA (25 mmol) in DMF. Yield: 59%; Colorless solid; ^{1}H NMR (500 MHz, DMSO-d_6) δ 11.20 (s, 1H), 10.55 (s, 1H), 8.93 – 8.15 (m, 1H), 5.99 (s, 1H), 3.17 (q, J = 6.7 Hz, 2H), 1.47 (p, J = 7.1 Hz, 2H), 1.27 (m, 4H), 0.86 (t, J = 6.9 Hz, 3H). ^{13}C NMR (126 MHz, DMSO-d_6) δ 164.31, 160.01, 150.89, 145.40, 99.74, 28.66, 28.35, 21.91, 13.99. LC-MS (m/z): positive mode 226 $[M+H]^{1+}$; Purity by HPLC UV (254 nm)-ESI-MS: 99.0%.

***N*-Hexyl-2,6-dioxo-1,2,3,6-tetrahydropyrimidine-4-carboxamide (83)**

Compound **83** was synthesized from the reaction of orotic acid (**78**, 10 mmol) with hexylamine (10 mmol) in the presence of HATU (10.5 mmol) and TEA (25 mmol) in DMF. Yield: 72%; Brown solid; ^{1}H NMR (500 MHz, DMSO-d_6) δ 11.20 (s, 1H), 10.56 (s, 1H), 8.72 (t, J = 5.7 Hz, 1H), 5.98 (s, 1H), 3.17 (td, J = 7.1, 5.6 Hz, 2H), 1.73 – 1.36 (m, 2H), 1.26 (dd, J = 5.5, 3.4 Hz, 6H), 1.00 – 0.58 (m, 3H). ^{13}C NMR (126 MHz, DMSO-d_6) δ 164.34, 160.04, 150.92, 145.45, 99.73, 31.05, 28.64, 26.15, 22.14, 14.03. LC-MS (m/z): positive mode 240 $[M+H]^{1+}$; Purity by HPLC UV (254 nm)-ESI-MS: 97.3%.

***N*-Octyl-2,6-dioxo-1,2,3,6-tetrahydropyrimidine-4-carboxamide (84)**

Compound **84** was synthesized from the reaction of orotic acid (**78**, 10 mmol) with octylamine (10 mmol) in the presence of HATU (10.5 mmol) and TEA (25 mmol) in DMF. Yield: 65%; Colorless solid; ^{1}H NMR (500 MHz, DMSO-d_6) δ 8.13 (s, 2H), 6.01 (s, 1H), 2.88 – 2.65 (m, 2H), 1.54 (tt, J = 7.9, 6.1 Hz, 2H), 1.37 – 1.05 (m, 10H), 1.03 – 0.64 (m, 3H). ^{13}C NMR (126 MHz, DMSO-d_6) δ 164.31, 159.90, 150.88, 145.29, 99.90, 31.35, 31.28, 28.78, 28.73, 28.62, 28.60, 27.03, 26.48,

26.00, 22.18, 14.05. LC-MS (m/z): positive mode 268 $[M+H]^{1+}$; Purity by HPLC UV (254 nm)-ESI-MS: 98.5%.

***N*-Nonyl-2,6-dioxo-1,2,3,6-tetrahydropyrimidine-4-carboxamide (85)**

Compound **85** was synthesized from the reaction of orotic acid (**78**, 10 mmol) with nonylamine (10 mmol) in the presence of HATU (10.5 mmol) and TEA (25 mmol) in DMF. Yield: 61%; Pale yellow solid; ^{1}H NMR (500 MHz, DMSO-d_6) δ 8.11 (s, 2H), 6.01 (s, 1H); 2.90 – 2.57 (m, 2H), 1.79 – 1.41 (m, 2H), 1.41 – 1.11 (m, 12H), 1.11 – 0.19 (m, 3H). ^{13}C NMR (126 MHz, DMSO-d_6) δ 164.41, 160.12, 99.63, 31.38, 29.02, 28.91, 28.82, 28.76, 28.69, 28.66, 27.08, 25.97, 22.20, 14.06. LC-MS (m/z): positive mode 282 $[M+H]^{1+}$; Purity by HPLC UV (254 nm)-ESI-MS: 97.0%.

Biological assays

The recombinant CHO cell line expressing the human GPR84 (CHO-hGPR84 cells) with a β-galactosidase fragment and arrestin containing the complementary fragment of the enzyme for performing β-arrestin recruitment assays (Pathhunter®) was purchased from DiscoverX (Fremont, CA). This cell line was used for the β-arrestin recruitment assays as well as for cAMP accumulation and radioligand binding assays. CHO-hGPR84 cells were cultured in F12 medium supplemented with 10 % FCS, 100 units/mL penicillin G, 100 µg/mL streptomycin, 800 µg/mL G 418, 300 µg/mL hygromycin B, and 1 % ultraglutamin (Invitrogen, Carlsbad, CA or Sigma-Aldrich, St. Louis, MO). Stock solutions of test compounds and of forskolin were prepared in DMSO. The final DMSO concentration in the assays did not exceed 1%. Data analysis was performed with GraphPad Prism (Version 6.02). Concentration-response data were fitted by non-linear regression to estimate EC_{50} values (Prism 6.02).

Membrane preparations

CHO-β-arrestin-hGPR84 cells were cultured in 150 cm^2 dishes in F12 medium supplemented with 10 % FCS, 100 units/mL penicillin G, 100 µg/mL streptomycin, 800 µg/mL G 418, 300 µg/mL

hygromycin B, and 1 % ultraglutamin. Confluent cells were washed with 5 mL of ice-cold PBS and the dishes were frozen at 80°C. Membranes were prepared by adding 1 mL of ice-cold 25 mM Tris buffer, pH 7.4 containing 0.32 M Sucrose, 1 mM EDTA, and protease inhibitors (1:100 dilution of the protease inhibitor cocktail, Sigma 8340) and scratching the cells off the previously frozen cell culture dishes. The collected cell suspension was homogenized with an Ultra Turrax and was subsequently centrifuged at 1,000 x g for 10 min at 4°C. The supernatant was carefully removed before being centrifuged at 48,000 x g for 30 min at 4°C. The obtained pellet was resuspended in 50 mM Tris buffer, pH 7.4, homogenized with an Ultra Turrax and centrifuged once again under the same conditions. The washing step was repeated once more. The final crude membrane pellet was resuspended in 50 mM Tris-HCl buffer (pH 7.4), homogenized in a glass/teflon homogenizer and stored at -80°C in 1-mL aliquots until further use. Protein concentrations were determined according to the method of Lowry.

McA-RH7777 cells and C6 glioma cells were provided by Prof. Dr. I. von Kügelgen (Institute of Pharmacology and Toxicology, University of Bonn, Bonn, Germany). For both cell lines DMEM (Dulbecco's Modified Eagle's Medium) medium supplemented with 10 % FCS, 100 units/mL penicillin G, 100 µg/mL streptomycin, and 1 % ultraglutamin was used. Human embryonic kidney (HEK)293 cells were purchased from the European Tissue Culture Collection (Salisbury, UK) and were cultured using MEM (Minimun essential Medium eagle) medium supplemented with 10 % FCS, 100 units/mL penicillin G, 100 µg/mL streptomycin, 1 % ultraglutamin, and 1 % NEAA (non essential amino acids solution). For HepG2 cells DMEM (Dulbecco's Modified Eagle's Medium), high glucose medium supplemented with 10 % FCS, 100 units/mL penicillin G and 100 µg/mL streptomycin was used. The preparation of the cell membranes from McA-RH7777, C6 glioma, HEK293 and HepG2 cells was performed as described above for CHO-β-arrestin-hGPR84 cells.

Bovine brains and livers were obtained from a local abattoir. Mouse and rat tissues were obtained from control animals that had been used for other experiments and were sacrificed.

The following membrane preparations were performed essentially as previously described: lymphocyte isolation and membrane preparations of the lymphocytes,[54] preparation of Jurkat-T cell membranes,[55] brain cortical membrane preparations and rat brain striatal membrane preparations,[56] membranes of 1321N1 astrocytoma cells.[57]

GPR84 radioligand binding assays

The radioligand binding assays were performed in a 96-well format. CHO cell membranes expressing the human GPR84 receptor (10 µg protein per vial) were incubated for 150 min at 25°C in 0.4 mL of a 50 mM Tris-HCl buffer (pH 7.4) containing 10 mM $MgCl_2$, 0.05 % fatty acid free BSA, 2 nM [^{3}H]**6** (60 Ci/mmol) and increasing concentrations of test compound. Nonspecific binding (NSB) was determined in the presence of 10 µM of **6**. Membrane-bound and free radioligand were separated by rapid filtration (GF/B-glass fiber filter) using a Brandel 96-channel cell harvester (Brandel, Gaithersburg, MD, USA) through Packard 96-well GF/B glass fibre filter plates. Filters were rinsed three times, 2 ml each, with ice-cold 50 mM Tris-HCl buffer, pH 7.4. Radioactivity of the 96-well filter plates was counted after 6 h of preincubation with 50 µL of Microscint-20 scintillation cocktail (Perkin Elmer, Rodgau, Germany). Data were analyzed using Graph Pad Prism Version 6.0 (San Diego, CA, USA). For the calculation of K_i values the Cheng-Prusoff equation and a K_D value of 2.08 nM was used. Three independent experiments, each in duplicates were performed. The unpaired t-test was used for statistical comparisons (*, $p<0.05$; **, $p<0.01$; ***$p<0.005$; ****$p<0.001$).

GPR84 cAMP accumulation assays

The cAMP assays were performed essentially as previously described.[24,26] In short, CHO-hGPR84 cells were stimulated with test compound dilutions (in DMSO, final concentration: 1%) or with

1 % DMSO alone (control) for 5 min at 37 °C. Subsequently, forskolin (10 μM) was added and the reaction mixtures were incubated for another 15 min at 37 °C. The reaction was stopped with hot (90 °C) lysis solution (4 mM EDTA, 0.01 % Triton X-100 in water). Accumulated cAMP levels were quantified by a radioactive assay using [^{3}H]cAMP (Perkin-Elmer, Rodgau, Germany). The forskolin-induced increase in cAMP concentration in the presence of agonist dilutions was expressed as percentage of the response to forskolin in the absence of agonists (% of control). Three independent experiments, each in duplicates were performed.

GPR84 β-arrestin recruitment assays

β-Arrestin assays were performed essentially as previously described.[24,26] Briefly, CHO-hGPR84 cells were incubated with compound dilutions (in DMSO, final concentration: 1%) for 90 min before adding the detection reagent (DiscoverX®). The reaction mixture was further incubated for 60 min at rt. The luminescence was measured using an NXT plate reader (Perkin-Elmer, Rodgau, Germany). Three independent experiments were performed, each in duplicates.

Three dimensional structure of the human GPR84

A homology model of the human GPR84 receptor was created using Modeller9.[58,59] The sequence of the human GPR84 was downloaded from the protein database, UniProtKB (Q9NQS5). The human GPR84 sequence comprised of 396 amino acid residues was submitted to Protein BLAST (Basic Local Alignment Search Tool) to search for the closest homologue in the Protein Data Bank (PDB). The templates identified using BLAST and the target sequence, the human GPR84, were aligned using the multiple sequence alignment tool, CLUSTALO.[60] Among the closest sequences identified, the human dopamine D3 receptor[45] contains a large intracellular loop 3 (ICL3) similar to GPR84. Thus, the human dopamine D3 receptor was selected as a template. The human GPR84 model was generated on the basis of the crystal structure of the human dopamine D3 receptor in complex with eticlopride (PDB ID: 3PBL).[44] The alignment between the human GPR84 and the

dopamine D3 receptor was visually interpreted and manually fixed for further improvement. Each model was optimized using the variable target function method (VTFM) with conjugate gradients (CG), followed by refinement using molecular dynamics (MD) with a simulated annealing (SA) method implemented in Modeller. In the dopamine D3 receptor the *N*-terminus and the ICL3 have not been crystallized and therefore modeling of these regions was not attempted. From the 100 generated models, the best homology model was selected on the basis of the Discrete Optimized Protein Energy (DOPE) score included in Modeller. The extracellular loop 2 (ECL2) of the best model was improved by using the loop modeller module implemented in Molecular Operating Environment (MOE 2014.09).[49] The putative orthosteric binding site was predicted by using the SiteFinder module in MOE2014.09. The overall structural quality was confirmed by a Ramachandran Plot, and sequence-structure compatibility of the model was ensured using PROSA II profile analysis.[46,48] The protonation of the final model was done using the Protonate3D algorithm in MOE2014.09 followed by minimization with a root mean square of 0.5 Å.

Molecular docking

The generated homology model of the human GPR84 was used for the docking procedure using AutoDock 4.2.[61] The AutoDockTools package was employed to generate the docking input files and to analyze the docking results. Three-dimensional energy scoring grids for a box of 60 × 60 × 60 points with a spacing of 0.375 Å were computed. The grids were centered based on the predicted orthosteric binding site of the receptor. For each ligand, 100 independent docking calculations using the *var*CPSO-ls algorithm from PSO@Autodock[62] implemented in AutoDock4.2 were performed and terminated after 500,000 evaluation steps. Parameters of *var*CPSO-ls algorithm, the cognitive and social coefficients c1 and c2, were set at 6.05 with 60 individual particles as a swarm size. Default values were used for all the other available parameters for the grid and docking

calculations. High scoring binding poses of lowest energy or more populated poses were selected for the analysis based on visual inspection.

AUTHOR INFORMATION

Corresponding Author

*For Prof. Dr. Christa E. Müller.: phone, +49-228-73-2301; fax, +49-228-73-2567; E-mail, christa.mueller@uni-bonn.de.

ORCID

Thanigaimalai Pillaiyar: 0000-0001-5575-8896

Vigneshwaran Namasivayam: 0000-0003-3031-3377

Christa E. Müller: 0000-0002-0013-6624

ACKNOWLEDGMENTS

This study was in part supported by the BMBF (Federal Ministery of Education and Research, Germany, BioPharma Neuroallianz). T.P. is grateful to the Alexander von Humboldt (AvH) foundation and to Bayer Pharma for supporting a postdoctoral fellowship. Expert technical contributions by Marion Schneider (LC-MS analyses), Sabine Terhart-Krabbe (NMR) and Annette Reiner (NMR) are gratefully acknowledged.

ABBREVIATIONS USED

cAMP, cyclic adenosine monophosphate; CHO, Chinese hamster ovary; DAD, diode array detector; DIM, diindolylmethane; DMF, *N*,*N'*-dimethylformamide; DMSO, dimethyl sulfoxide; ESI, electrospray ionization; FFA/R, free fatty acid/receptor; GPCR, G protein-coupled receptor; GPR, G protein-coupled receptor; HEK, Human embryonic kidney; HPLC, high performance

liquid chromatography; LC-MS, liquid chromatography-mass spectrometry; MAPK, mitogen-activated protein kinase; M/L/SCFA, medium/long/short chain fatty acid; NFκB, nuclear factor kappa-light-chain-enhancer of activated B cells; NMR, nuclear magnetic resonance; SAR, structure-activity relationship; THF, tetrahydrofuran; TLC, thin layer chromatography

Notes

The authors declare no competing financial interest.

ASSOCIATED CONTENT

Supporting Information

Mass spectrometric analysis of [^{3}H]**6** (**A**) and of the unlabeled reference compound **6** (**B**); Radiochemical purity of [^{3}H]**6** determined by HPLP-UV (254 nm); Product specification sheet of [^{3}H]**6**; Specific binding of [^{3}H]**6** to CHO-K1 and CHO-hGPR17 membrane preparations; effects of sodium ions on binding of [^{3}H]**6**. NMR and HPLC-UV/MS data for selected compounds. Overall sequence alignment of the human GPR84 and the human dopamine D3 receptor; Ramachandran diagram of the human GPR84 model; Sequence-structure compatibility of the human GPR84 model; docked poses of compounds **3** and **7** in the binding site of the GPR84 model; competition binding experiments of compounds **6** and **7** at native human and rodent tissues and cell lines.

Molecular SMILES strings and EC_{50} values (CSV).

Accession Codes

The authors will release the atomic coordinates of the homology model of the human GPR84 based on the X-ray structure of the human dopamine D3 receptor (PDB ID: 3PBL) upon article publication.

REFERENCES

(1) Wittenberger, T.; Schaller, H. C.; Hellebrand, S. An expressed sequence tag (EST) data mining strategy succeeding in the discovery of new Gprotein-coupled receptors. *J. Mol. Biol.* **2001**, *307*, 799-813.

(2) Yousefi, S.; Cooper, P. R.; Potter, S. L.; Mueck, B.; Jarai, G. Cloning and expression analysis of a novel G protein-coupled receptor selectively expressed on granulocytes. *J. Leukoc. Biol.* **2001**, *69*, 1045-1052.

(3) Venkataraman, C.; Kuo, F. The Gprotein-coupled receptor, GPR84 regulates IL-4 production by T lymphocytes in response to CD3 crosslinking. *Immunol. Lett.* **2005**, *101*, 144-153.

(4) Wang, J.; Wu, X.; Simonavicius, N.; Tian, H.; Ling, L. Medium chain fatty acids as ligands for orphan G protein-coupled receptor GPR84. *J. Biol. Chem.* **2006**, *281*, 34457-34464.

(5) Bouchard, C.; Pagé, J.; Bédard, A.; Tremblay, P.; Vallières, L. G protein-coupled receptor 84, a microglia-associated protein expressed in neuroinflammatory conditions. *Glia* **2007**, *55*, 790-800.

(6) Recio, C.; Lucy, D.; Purvis, G. S. D.; Iveson, P.; Zeboudj, L.; Iqbal, A. J.; Lin, D.; O'Callaghan, C.; Davison, L.; Griesbach, E.; Russell, A. J.; Wynne, G. M.; Dib, L.; Monaco, C.; Greaves, D. R. Activation of the immune-metabolic receptor GPR84 enhances inflammation and phagocytosis in macrophages. *Front. Immunol.* **2018**, *9*, 1419.

(7) Suzuki, M.; Takaishi, S.; Nagasaki, M.; Onozawa, Y.; Iino, I.; Maeda, H.; Komai, T.; Oda, T. Medium-chain fatty acid-sensing receptor, GPR84, is a proinflammatory receptor. *J. Biol. Chem.* **2013**, *288*, 10684 -10691.

(8) Gaidarov, I.; Anthony, T.; Gatlin, J.; Chen, X.; Mills, D.; Solomon, M.; Han, S.; Semple, G.; Unett, D. J. Embelin and its derivatives unravel the signaling, proinflammatory and antiatherogenic properties of GPR84 receptor. *Pharmacol. Res*. **2018**, *131*, 185-198.

(9) Sundqvist, M.; Christenson, K.; Holdfeldt, A.; Gabl, M.; Mårtensson, J.; Björkman, L.; Dieckmann, R.; Dahlgren, C.; Forsman, H. Similarities and differences between the responses induced in human phagocytes through activation of the medium chain fatty acid receptor GPR84 and the short chain fatty acid receptor FFA2R. *Biochim. Biophys. Acta* **2018**, *1865*, 695-708.

(10) Abdel-Aziz, H.; Schneider, M.; Neuhuber, W.; Kassem, A. M.; Khailah, S.; Muller, J.; Gamaleldeen, H.; Khairy, A.; Khayyal, M. T.; Shcherbakova, A.; Efferth, T.; Ulrich-Merzenich, G. GPR84 and TREM-1 signaling contribute to the pathogenesis of reflux esophagitis. *Mol. Med*. **2015**, *21*, 1011-1024.

(11) Dupont, S.; Arijs, I.; Blanque, R.; Laukens, D.; Nys, K.; Ceccotti, M. C.; Merciris, D.; De Vos, S.; Mate, O.; Parent, I.; De Vriendt, V.; Labeguere, F.; Galien, R.; Devos, M.; Rutgeerts, P.; Vandeghinste, N.; Vermeire, S.; Brys, R. GPR84 inhibition as a novel therapeutic approach in IBD: mechanistic and translational studies. *J. Crohns Colitis* **2015**, *9*, S92-S93.

(12) Nicol, L. S.; Dawes, J. M.; La Russa, F.; Didangelos, A.; Clark, A. K.; Gentry, C.; Grist, J.; Davies, J. B.; Malcangio, M.; McMahon, S. B. The role of Gprotein-receptor 84 in experimental neuropathic pain. *J. Neurosci.* **2015**, *35*, 8959-8969.

(13) Audoy-Remus, J.; Bozoyan, L.; Dumas, A.; Filali, M.; Cynthia, L.; Lacroix, S.; Rivest, S.; Tremblay, M. E.; Vallieres, L. GPR84 deficiency reduces microgliosis, but accelerates dendritic degeneration and cognitive decline in a mouse model of Alzheimer's disease. *Brain, Behav., Immun.* **2015**, *46*, 112-120.

(14) Nagasaki, H.; Kondo, T.; Fuchigami, M.; Hashimoto, H.; Sugimura, Y.; Ozaki, N.; Arima, H.; Ota, A.; Oiso, Y.; Hamada, Y. Inflammatory changes in adipose tissue enhance expression of GPR84, a medium-chain fatty acid receptor: TNFα enhances GPR84 expression in adipocytes. *FEBS Lett.* **2012**, *586*, 368-372.

(15) Wellendorph, P.; Johansen, L. D.; Bräuner-Osborne, H. Molecular pharmacology of promiscuous seven transmembrane receptors sensing organic nutrients. *Mol. Pharmacol*. **2009**, *76*, 453-465.

(16) Yonezawa, T.; Kurata, R.; Yoshida, K.; Murayama, M. A.; Cui, X.; Hasegawa, A. Free fatty acids-sensing G protein-coupled receptors in drug targeting and therapeutics. *Curr. Med. Chem*. **2013**, *20*, 3855-3871.

(17) Miyamoto, J.; Hasegawa, S.; Kasubuchi, M.; Ichimura, A.; Nakajima, A.; Kimura, I. Nutritional signaling via free fatty acid receptors. *Int. J. Mol. Sci.* **2016**, *17*, 450-462.

(18) Dietrich, P. A.; Yang, C.; Leung, H. H. L.; Lynch, J. R.; Gonzales, E.; Liu, B.; Haber, M.; Norris, M. D.; Wang, J. L.; Wang, J. Y. GPR84 sustains aberrant beta-catenin signaling in leukemic stem cells for maintenance of MLL leukemogenesis. *Blood* **2014**, *124*, 3284-3294.

(19) Park, J. W.; Yoon, H. J.; Kang, W. Y.; Cho, S.; Seong, S. J.; Lee, H. W.; Yoon, Y. R.; Kim, H. J. G protein-coupled receptor 84 controls osteoclastogenesis through inhibition of NF-κB and MAPK signaling pathways. *J. Cell. Physiol.* **2018**, *233*, 1481-1489.

(20) Gagnon, L.; Leduc, M.; Thibodeau, J. F.; Zhang, M. Z.; Grouix, B.; Bournet- Sarra, F.; Gagnon, W.; Hince, K.; Tremblay, M.; Geerts, L.; Kennedy, C. R. J.; Hebert, R. L.; Gutsol, A.; Holterman, C. E.; Kamto, E.; Gervais, L.; Ouboudinar, J.; Richard, J.; Felton, A.; Laverdure, A.; Simard, J. C.; Letournau, S.; Cloutier, M. P.; Leblond, F. A.; Abbot, S. D.; Penney, C.; Duceppe, J. S.; Zacharie, B.; Dupuis, J.; Calderone, A.; Nguyen, Q. T.; Harris, R. C.; Laurin, P. A newly discovered antifibrotic pathway regulated by two fatty acid receptors. *Am. J. Pathol*. **2018**, *188*, 1132-1148.

(21) Southern, C.; Cook, J. M.; Neetoo-Isseljee, Z.; Taylor, D. L.; Kettleborough, C. A.; Merritt, A.; Bassoni, D. L.; Raab, W. J.; Quinn, E.; Wehrman, T. S.; Davenport, A. P.; Brown, A. J.; Green, A.; Wigglesworth, M. J.; Rees, S. Screening β-arrestin recruitment for the identification of natural ligands for orphan Gprotein-coupled receptors. *J. Biomol. Screen.* **2013**, *18*, 599-609.

(22) Nikaido, Y.; Koyama, Y.; Yoshikawa, Y.; Furuya, T.; Takeda, S. Mutation analysis and molecular modeling for the investigation of ligand-binding modes of GPR84. *J. Biochem*. **2015**, *157*, 311-320.

(23) Kaspersen, M. H.; Jenkins, L.; Dunlop, J.; Milligan, G.; Ulven, T. Succinct synthesis of saturated hydroxy fatty acids and in vitro evaluation of all hydroxylauric acids on FFA1, FFA4 and GPR84. *MedChemComm.* **2017**, *8*, 1360-1365.

(24) Pillaiyar, T.; Köse, M.; Namasivayam, V.; Sylvester, K.; Borges, G.; Thimm, D.; von Kügelgen, I.; Müller, C.E. 6-(Ar)Alkylamino-substituted uracil derivatives: lipid mimetics with potent activity at the orphan G protein-coupled receptor 84 (GPR84). *ACS Omega* **2018**, *3*, 3365-3383.

(25) Mahmud, Z. A.; Jenkins, L.; Ulven, T.; Labeguere, F.; Gosmini, R.; De Vos, S.; Hudson, B. D.; Tikhonova, I. G.; Milligan, G. Three classes of ligands each bind to distinct sites on the orphan G protein-coupled receptor GPR84. *Sci. Rep.* **2017**, *7*, 17953-17967.

(26) Pillaiyar, T.; Köse, M.; Sylvester, K.; Weighardt, H.; Thimm, D.; Borges, G.; Förster, I.; von Kügelgen, I.; Müller, C. E. Diindolylmethane derivatives: potent agonists of the immunostimulatory orphan G protein-coupled receptor GPR84. *J. Med. Chem.* **2017**, *60*, 3636-3655.

(27) Hakak, Y.; Unett, D. J.; Gatlin, J.; Liaw, C. W. Human G Protein-Coupled Receptor and Modulators Thereof for the Treatment of Atherosclerosis and Atherosclerotic Disease and for the Treatment of Conditions Related to MCP-1 Expression. International Patent application WO2007027661, 2007.

(28) Zhang, Q.; Yang, H.; Li, J.; Xie, X. Discovery and characterization of a novel small molecule agonist for medium chain free fatty acid receptor GPR84. *J. Pharmacol. Exp. Ther.* **2016**, *357*, 337-344

(29) Liu, Y.; Zhang, Q.; Chen, L. H.; Yang, H.; Lu, W.; Xie, X.; Nan, F. J. Design and synthesis of 2 alkylpyrimidine-4,6-diol and 6 alkylpyridine-2,4-diol as potent GPR84 agonists. *ACS Med. Chem. Lett.* **2016**, *7*, 579-583.

(30) Takeda, S.; Yamamoto, A.; Okada, T.; Matsumura, E.; Nose, E.; Kogure, K.; Kojima, S.; Haga, T. Identification of surrogate ligands for orphan G protein-coupled receptors. *Life Sci*. **2003**, *74*, 367-377.

(31) Marques, M.; Laflamme, L.; Benassou, I.; Cissokho, C.; Guillemette, B.; Gaudreau, L. Low levels of 3,3′-diindolylmethane activate estrogen receptor α and induce proliferation of breast cancer cells in the absence of estradiol. *BMC Cancer* **2014**, *14*, 524-533.

(32) Yin, X. F.; Chen, J.; Mao, W.; Wang, Y. H.; Chen, M. H. A selective aryl hydrocarbon receptor modulator 3,3'-diindolylmethane inhibits gastric cancer cell growth. *J. Exp. Clin. Cancer Res.* **2012**, *31*, 31-46.

(33) Mancini, S. J.; Mahmud, Z. A.; Jenkins, L.; Bolognini, D.; Newman, R.; Barnes, M.; Edye, M. E.; McMahon, S. B.; Tobin, A. B.; Milligan, G. On-target and off-target effects of novel orthosteric and allosteric activators of GPR84. *Sci. Rep.* **2019**, 9, 1861.

(34) Labeguere, F. Luke, A.; Gregory, N.; Laurent, S.; Stephen, F. Novel Dihydropyrimidinoisoquinolinones and Pharmaceutical Compositions Thereof for the Treatment of Inflammatory Disorders. WO 2013/092791A1, 2014.

(35) Niedernberg, A.; Tunaru, S.; Blaukat, A.; Harris, B.; Kostenis, E. Comparative analysis of functional assays for characterization of agonist ligands at G protein-coupled receptors. *J. Biomol. Screen*. **2003**, *8*, 500-510.

(36) Niedernberg, A.; Blaukat, A.; Schöneberg, T.; Kostenis, E. Regulated and constitutive activation of specific signalling pathways by the human S1P5 receptor. *Br. J. Pharmacol.* **2003**, *138*, 481-493.

(37) Mitsunobu, O. The use of diethyl azodicarboxylate and triphenylphosphine in synthesis and transformation of natural products. *Synthesis* **1981**, 1-28.

(38) Liu, W.; Chun, E.; Thompson, A. A.; Chubukov, P.; Xu, F.; Katritch, V.; Han, G.W.; Roth, C. B.; Heitman, L. H.; IJzerman, A. P.; Cherzov, V.; Stevens, R. C. Structural basis for allosteric regulation of GPCRs by sodium ions. *Science* **2012**, *337*, 232-236.

(39) Thimm, D.; Funke, M.; Meyer, A.; Müller, C. E. 6-Bromo-8-(4-[^{3}H]methoxy-benzamido)-4-oxo-4H-chromene-2-carboxylic acid ([^{3}H]PSB-13253): a powerful tool for studying orphan G protein-coupled receptor GPR35. *J. Med. Chem.* **2013**, *56*, 7084-7099.

(40) Köse, M.; Ritter, K.; Thiemke, K.; Gillard, M.; Kostenis, E.; Müller, C. E. Development of [(^{3})H]2-carboxy-4,6-dichloro-1H-indole-3-propionic acid ([(^{3})H]PSB-12150): a useful tool for studying GPR17. *ACS Med. Chem. Lett.* **2014**, *5*, 326-330.

(41) Van der Westhuizen, E. T.; Valant, C.; Sexton, P. M.; Christopoulos, A. Endogenous allosteric modulators of G protein-coupled receptors. *J. Pharmacol. Exp. Ther.* **2015**, 353, 246-260.

(42) Shrestha, R.; Hui, S. P.; Imai, H.; Hashimoto, S.; Uemura, N.; Takeda, S.; Fuda, H.; Suzuki, A.; Yamaguchi, S.; Hirano, K.; Chiba, H. Plasma capric acid concentrations in healthy subjects determined by high-performance liquid chromatography. *Ann. Clin. Biochem.* **2015**, *52*, 588-596.

(43) Altschul, S.F.; Gish, W.; Miller, W.; Myers, E. W.; Lipman, D. J. Basic local alignment search tool. *J. Mol. Biol.* **1990**, *215*, 403-410.

(44) Chien, E. Y. T.; Liu, W.; Zhao, Q.; Katritch, V.; Han, G. W.; Hanson, M. A.; Shi, L.; Newman, A. H.; Javitch, J. A.; Cherezov, V.; Stevens, R. C. Structure of the human dopamine D3 receptor in complex with a D2/D3 selective antagonist. *Science* **2010**, *330*, 1091-1095.

(45) Tikhonova, I. G. Application of GPCR structures for modelling of free fatty acid receptors. *Handb. Exp. Pharmacol.* **2017**, *236*, 57-77.

(46) Ramachandran, G. N.; Ramakrishnan, C.; Sasisekharan, V. Stereochemistry of polypeptide chain configurations. *J. Mol. Biol.* **1963**, *7*, 95-99.

(47) Lovell, S. C.; Davis, I. W.; Arendall, W. B. 3rd; de Bakker, P. I.; Word, J. M.; Prisant, M. G.; Richardson, J. S.; Richardson, D. C. Structure validation by Calpha geometry: phi, psi and Cbeta deviation. *Proteins* **2003,** *50*, 437-450.

(48) Wiederstein, M.; Sippl, M. J. ProSA-web: Interactive web service for the recognition of errors in three-dimensional structures of proteins. *Nucleic Acids Res.* **2007**, *35*, W407–W410.

(49) Molecular Operating Environment (MOE), 2014.09, Chemical Computing Group Inc., 1010 Sherbooke St. West, Suite #910, Montreal, QC, Canada, H3A 2R7, **2016**.

(50) Więcek, M.; Kottke, T.; Ligneau, X.; Schunack, W.; Seifert, R.; Stark, H.; Handzlik, J.; Kieć-Kononowicz, K. N-Alkenyl and cycloalkyl carbamates as dual acting histamine H3 and H4 receptor ligands. *Bioorg. Med. Chem.* **2011**, *19*, 2850-2858.

(51) Goulet, J. L.; Holmes, M. A.; Hunt, J. A.; Mills, S. G.; Parsons, W. H.; Sinclair, P. J.; Zaller, D. M. Src Kinase Inhibitor Compounds. WO 2001000207 A1, 2001.

(52) Novotna, Z.; Koos, M.; Matulova, M. Preparation and characterization of 2-alkylthio-4-(4-bromomethylbenzoyloxy)-6-methylpyrimidines. *Chemical Papers* **1991**, *45*, 651-656.

(53) Obrecht, D.; Ermert, P.; Luther, A.; Eberle, M.; Bachmann, F. Preparation of 2,4,6-Trisubstituted Pyrimidine Derivatives as Apoptosis Inducers for the Treatment of Neoplastic and Autoimmune Diseases. WO 2004087679 A1, 2004.

(54) Schiedel, A. C.; Lacher, S. K.; Linnemann, C.; Knolle, P. A.; Müller, C. E. Antiproliferative effects of selective adenosine receptor agonists and antagonists on human lymphocytes: evidence for receptor-independent mechanisms. *Purinergic Signal*. **2013**, *9*, 351-365.

(55) Hinz, S.; Navarro, G.; Borroto-Escuela, D.; Seibt, B. F.; Ammon, Y. C.; de Filippo, E.; Danish, A.; Lacher, S. K.; Červinková, B.; Rafehi, M.; Fuxe, K.; Schiedel, A. C.; Franco, R.; Müller, C. E. Adenosine A_{2A} receptor ligand recognition and signaling is blocked by A_{2B} receptors. *Oncotarget* **2018**, *9*, 13593-13611.

(56) Köse, M.; Gollos, S.; Karcz, T.; Fiene, A.; Heisig, F.; Behrenswerth, A.; Kieć-Kononowicz, K.; Namasivayam, V.; Müller, C. E. Fluorescent-labeled selective adenosine A_{2B} receptor antagonist enables competition binding assay by flow cytometry. *J. Med. Chem.* **2018**, *61*, 4301-4316.

(57) Abdelrahman, A.; Namasivayam, V.; Hinz, S.; Schiedel, A. C.; Köse, M.; Burton, M.; El-Tayeb, A.; Gillard, M.; Bajorath, J.; de Ryck, M.; Müller, C. E. Characterization of P2X4 receptor agonists and antagonists by calcium influx and radioligand binding studies. *Biochem. Pharmacol.* **2017**, *125*, 41-54.

(58) Sali, A.; Blundell, T. L. Comparative protein modelling by satisfaction of spatial restraints. *J. Mol. Biol.* **1993**, 234, 779-815.

(59) Webb, B.; Sali, A. Protein structure modeling with MODELLER. *Methods Mol. Biol.* **2014**, *1137*, 1-15.

(60) Sievers, F.; Wilm, A.; Dineen, D.; Gibson, T. J.; Karplus, K.; Li, W.; Lopez, R.; McWilliam, H.; Remmert, M.; Söding, J.; Thompson, J. D.; Higgins, D.G. Fast, scalable generation of high-quality protein multiple sequence alignments using Clustal Omega. *Mol. Syst. Biol.* **2011**, *7*, 539.

(61) Morris, G. M.; Huey, R.; Lindstrom, W.; Sanner, M. F.; Belew, R. K.; Goodsell, D. S.; Olson, A. J. AutoDock4 and AutoDockTools4: automated docking with selective receptor flexibility. *J. Comput. Chem.* **2009**, *30,* 2785-2791.

(62) Namasivayam, V.; Gunther, R. pso@autodock: a fast flexible molecular docking program based on Swarm intelligence. *Chem. Biol. Drug Des.* **2007**, *70*, 475-484.

TOC

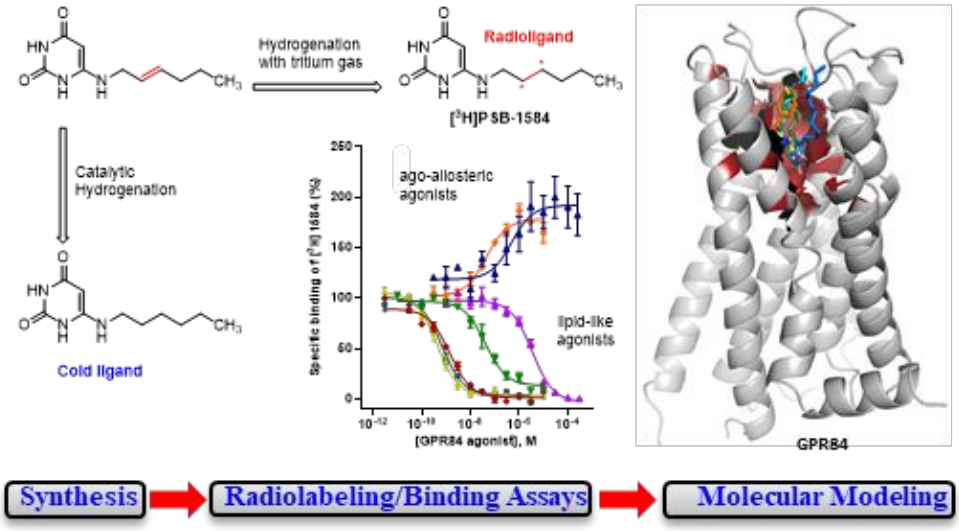
Hydrogenation with tritium gas
Radioligand
[3H]PSB-1584
Catalytic Hydrogenation
Cold ligand
ago-allosteric agonists
lipid-like agonists
Specific binding of [3H] 1584 (%)
[GPR84 agonist], M
GPR84
Synthesis
Radiolabeling/Binding Assays
Molecular Modeling